Calculation of a hydrogen atom photoionization in a strong magnetic field by using the angular oblate spheroidal functions

2007 J. Phys. A: Math. Theor. 40 11485

(http://iopscience.iop.org/1751-8121/40/38/004)

IOP Publishing Journal of Physics A: Mathematical and Theoretical

J. Phys. A: Math. Theor. **40** (2007) 11485–11524 doi:10.1088/1751-8113/40/38/004

Calculation of a hydrogen atom photoionization in a strong magnetic field by using the angular oblate spheroidal functions

O Chuluunbaatar[1], A A Gusev[1], V L Derbov[2], M S Kaschiev[3], L A Melnikov[2], V V Serov[2] and S I Vinitsky[1]

[1] Joint Institute for Nuclear Research, Dubna, Moscow Region 141980, Russia
[2] Saratov State University, Russia
[3] Institute of Mathematics and Informatics, BAS, Sofia, Bulgaria

Received 7 June 2007, in final form 9 August 2007
Published 4 September 2007
Online at stacks.iop.org/JPhysA/40/11485

Abstract

A new efficient method for calculating the photoionization of a hydrogen atom in a strong magnetic field is developed based on the Kantorovich approach to the parametric boundary problems in spherical coordinates using the orthogonal basis set of angular oblate spheroidal functions. The progress as compared with our previous paper (Dimova M G, Kaschiev M S and Vinitsky S I 2005 *J. Phys. B: At. Mol. Opt. Phys.* **38** 2337–52) consists of the development of the Kantorovich method for calculating the wavefunctions of a continuous spectrum, including the quasi-stationary states imbedded in the continuum. Resonance transmission and total reflection effects for scattering processes of electrons on protons in a homogenous magnetic field are manifested. The photoionization cross sections found for the ground and excited states are in good agreement with the calculations by other authors and demonstrate correct threshold behavior. The estimates using the calculated photoionization cross section show that due to the quasi-stationary states the laser-stimulated recombination may be enhanced by choosing the optimal laser frequency.

PACS numbers: 31.15.Ja, 31.15.Pf, 34.50.Pi, 32.80.Fb

1. Introduction

In recent decades the dynamics of transient processes in magnetic traps, such as excitation, de-excitation, ionization, recombination of ions and atoms, became a subject of intense experimental and theoretical studies [1–4]. Recently a new mechanism of formation of metastable positive-energy atoms via quasi-stationary states [5] due to the magnetic field was revealed. The most complicated case when the magnetic energy is comparable to that of Coulomb interaction requires new approaches to provide really stable numerical schemes

for the states of both discrete and continuous spectra, including the quasi-stationary states, analogous to the well-known doubly excited states of a helium atom [6–10]. In the known approaches serious problems arise, for example, concerned with reproducing true threshold behavior in the variational complex rotation method [8, 11] or with constructing efficient and stable numerical schemes [11]. In doing so, this method does not describe the difference in physical asymptotics of scattering states for a different choice of a gauge of magnetic field [12]. The **R**-matrix approach [13–16] using the combined nonorthogonal basis of Landau and Sturmian functions in both cylindrical and spherical coordinates leads to the ill-conditioned matrix problems [6, 17]. The method of diabatic sector basis functions requires a huge interval for the integration of the closed set of radial equations, because the overlap matrix between the pure physical asymptotic solutions in cylindrical coordinates and the numerical basis functions at large r can be calculated only numerically [7, 10]. The Kantorovich method (KM) [18] has been shown to provide strong mathematical background for consequent development of the adiabatic approach in spherical coordinates [19] using the orthogonal basis set of angular oblate spheroidal functions (AOSF) [20]. This approach yields stable calculation schemes for boundary problems, however, heretofore it has been elaborated only for the discrete spectrum problem [9].

In the present paper we develop the KM (i.e., the reduction of the boundary problem for elliptical partial differential equation in a 2D domain to a regular boundary problem for a set of ordinary second-order differential equations with variable coefficients with the boundary conditions of the third kind) in the form, appropriate for **R**-matrix calculations of the continuous spectrum and photoionization of atomic hydrogen in a strong magnetic field [21]. The solution depending on the radial variable r and the angular variable $\eta = \cos\theta = z/r$ with fixed values of the magnetic quantum number m and the z-parity σ is expanded using the basis set of the AOSF, which is orthogonal at fixed values of the radial variable. A matter of principle in the implementation of KM is how to calculate the matrix of the variable coefficients, expressed as angular integrals involving the derivatives of the angular functions with respect to a parameter, keeping the accuracy the same as for the angular functions themselves. This is achieved by calculating the mentioned derivatives as solutions of the inhomogenous boundary problem that results from differentiation of the ordinary second-order differential equation for the spheroidal functions with respect to the parameter and the corresponding algebraic eigenvalue problem, for which a stable symbolic-numerical algorithm is developed [22, 23]. The stability of the computational scheme is achieved using the fact that at small r (in the vicinity of pair collision point) the angular functions turn into the associated Legendre polynomials, while at large r near $\eta = \pm 1$ they turn into the associated Laguerre functions [24, 25]. This makes it possible to construct asymptotic expansions in powers of r^{-2}, necessary for computer-accuracy calculation of the basis set of functions at all values of the parameter r. Substantial economy of computer resource in the numerical solution of the boundary problem for the set of radial equations is achieved by decreasing the integration interval $0 \leqslant r \leqslant r_{\max}$. With this aim in the present paper for large $r \geqslant r_{\max}$ new asymptotic expansions of the fundamental solutions of the radial equations are constructed in the basis of linear combinations of Coulomb regular and irregular functions and their derivatives. The corresponding matrix of asymptotic expansions of fundamental solutions is derived in the analytic form and is related to the overlap matrix between the physical asymptotic form of fundamental solutions in the cylindrical coordinates, $z = r\cos\theta$, $\rho = r\sin\theta$ and the asymptotic form of the basis functions of the independent variable $\eta = \cos\theta$ at large values of r. The presented recurrence relations for expressing this matrix in the analytic form are the key to calculating the reaction matrix **K** via the matrix of logarithmic derivative of the radial solution in the joining point of numerical and asymptotic solutions in the inner and outer regions. The capabilities of the elaborated method and the

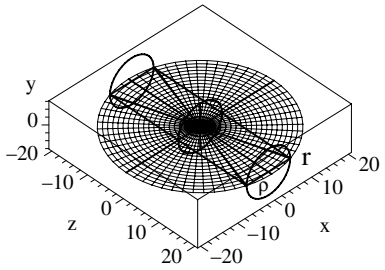

Figure 1. Projections of cylindrical and spherical coordinate systems in the zx plane for a hydrogen atom or scattering of an electron with a proton in a homogenous magnetic field $\vec{B} = (0, 0, B)$.

computational scheme are demonstrated by the example of photoionization cross section of a hydrogen atom in the magnetic field. Using the previously derived relation between the photoionization cross section and the laser-induced radiative recombination rate, it is shown that the latter can be increased by tuning the laser frequency to resonances that arise due to quasi-stationary states.

The paper is organized as follows. In section 2 the 2D-eigenvalue problem for the Schrödinger equation, describing a hydrogen atom in an axially symmetric magnetic field, is considered in the cylindrical coordinates together with the appropriate classification of states. The reduction of the 2D-eigenvalue problem to a 1D-eigenvalue problem for a set of closed longitude equations via both the Kantorovich and Galerkin methods is described briefly. It is shown that the Galerkin expansion follows from the Kantorovich expansion at $z \to \pm\infty$. In section 2.3 the relation between the function with given parity and the function having the physical scattering asymptotic form in the cylindrical coordinates is established. In section 3 the same problem as in section 2 is considered in the spherical coordinates. The reduction of the 2D-eigenvalue problem to a 1D-eigenvalue problem for a set of closed radial equations via four steps of the KM is described briefly in section 3.1. The asymptotic forms of the matrix element and radial solutions are considered in sections 3.2–3.5. The asymptotic expressions using regular and irregular Coulomb functions needed to find the solutions and the reaction matrix by means of the **R**-matrix method are presented in section 3.6. The correspondence of asymptotic total wavefunctions at large r and $|z|$ is shown explicitly in section 3.7. The method is applied to the ionization of low-lying states of a hydrogen atom in section 4. In section 5 the numerical results obtained within the framework of the finite-element method are discussed. The estimates of the laser-induced recombination rate based on the calculated photoionization cross sections are also presented. In conclusion we outline the perspectives of further applications of this approach. The detailed analysis of asymptotic calculations is given in appendix A, B and C.

2. Statement of the problem in cylindrical coordinates

In the cylindrical coordinates (ρ, z, φ) (see figure 1) the wavefunction

$$\hat{\Psi}(\rho, z, \varphi) = \Psi(\rho, z)\frac{\exp(\imath m\varphi)}{\sqrt{2\pi}} \tag{1}$$

of a hydrogen atom in an axially symmetric magnetic field $\vec{B} = (0, 0, B)$ satisfies the 2D Schrödinger equation

$$-\frac{\partial^2}{\partial z^2}\Psi(\rho, z) + \left(\hat{A}_c - \frac{2Z}{\sqrt{\rho^2 + z^2}}\right)\Psi(\rho, z) = \epsilon\Psi(\rho, z), \tag{2}$$

$$\hat{A}_c = -\frac{1}{\rho}\frac{\partial}{\partial\rho}\rho\frac{\partial}{\partial\rho} + \frac{m^2}{\rho^2} + m\gamma + \frac{\gamma^2\rho^2}{4}, \tag{3}$$

in the region Ω_c: $0 < \rho < \infty$ and $-\infty < z < \infty$. Here $m = 0, \pm 1, \ldots$ is the magnetic quantum number, $\gamma = B/B_0$, $B_0 \cong 2.35 \times 10^5 T$ is a dimensionless parameter which determines the field strength B. We use the atomic units (au) $\hbar = m_e = e = 1$ and assume the mass of the nucleus with a charge Z to be infinite. In these expressions $\epsilon = 2E$ is the twice energy (expressed in Rydbergs, 1 Ry $= (1/2)$ au) of the bound state $|m\sigma\rangle$ with fixed values of m and z-parity $\sigma = \pm 1$ and $\Psi(\rho, z) \equiv \Psi^{m\sigma}(\rho, z) = \sigma\Psi^{m\sigma}(\rho, -z)$ is the corresponding wavefunction. The boundary conditions in each $m\sigma$ subspace of the full Hilbert space have the form

$$\lim_{\rho\to 0}\rho\frac{\partial\Psi(\rho, z)}{\partial\rho} = 0, \qquad \text{for} \quad m = 0, \qquad \text{and} \qquad \Psi(0, z) = 0, \quad \text{for} \quad m \neq 0, \tag{4}$$

$$\lim_{\rho\to\infty}\Psi(\rho, z) = 0. \tag{5}$$

The wavefunction of the discrete spectrum obeys the asymptotic boundary condition. Approximately this condition is replaced by the boundary condition of the first type at large, but finite $|z| = z_{\max} \gg 1$, namely,

$$\lim_{z\to\pm\infty}\Psi(\rho, z) = 0 \quad \rightarrow \quad \Psi(\rho, \pm z_{\max}) = 0. \tag{6}$$

These functions satisfy the additional normalization condition

$$\int_{-z_{\max}}^{z_{\max}}\int_0^\infty |\Psi(\rho, z)|^2\rho\,\mathrm{d}\rho\,\mathrm{d}z = 1. \tag{7}$$

The asymptotic boundary condition for the continuum wavefunction will be considered in section 2.3.

2.1. Kantorovich expansion

Consider a formal expansion of the partial solution $\Psi_i^{Em\sigma}(\rho, z)$ of equations (2)–(5), corresponding to the eigenstate $|m\sigma i\rangle$, expanded in the finite set of one-dimensional basis functions $\left\{\hat{\Phi}_j^m(\rho; z)\right\}_{j=1}^{j_{\max}}$

$$\Psi_i^{Em\sigma}(\rho, z) = \sum_{j=1}^{j_{\max}}\hat{\Phi}_j^m(\rho; z)\hat{\chi}_j^{(m\sigma i)}(E, z). \tag{8}$$

In equation (8) the functions $\hat{\chi}^{(i)}(z) \equiv \hat{\chi}^{(m\sigma i)}(E, z)$, $(\hat{\chi}^{(i)}(z))^T = (\hat{\chi}_1^{(i)}(z), \ldots, \hat{\chi}_{j_{\max}}^{(i)}(z))$ are unknown and the surface functions $\hat{\mathbf{\Phi}}(\rho; z) \equiv \hat{\mathbf{\Phi}}^m(\rho; z) = \hat{\mathbf{\Phi}}^m(\rho; -z)$, $(\hat{\mathbf{\Phi}}(\rho; z))^T = (\hat{\Phi}_1(\rho; z), \ldots, \hat{\Phi}_{j_{\max}}(\rho; z))$ form an orthonormal basis for each value of the variable z which is treated as a parameter.

In the Kantorovich approach the wavefunctions $\hat{\Phi}_j(\rho; z)$ and the potential curves $\hat{E}_j(z)$ (in Ry) are determined as the solutions of the following one-dimensional parametric eigenvalue problem

$$\left(\hat{A}_c - \frac{2Z}{\sqrt{\rho^2 + z^2}}\right)\hat{\Phi}_j(\rho; z) = \hat{E}_j(z)\hat{\Phi}_j(\rho; z), \tag{9}$$

with the boundary conditions

$$\lim_{\rho\to 0} \rho\frac{\partial\hat{\Phi}_j(\rho; z)}{\partial\rho} = 0, \qquad \text{for} \quad m = 0, \quad \text{and} \quad \hat{\Phi}_j(0; z) = 0, \qquad \text{for} \quad m \neq 0, \tag{10}$$

$$\lim_{\rho\to\infty} \hat{\Phi}_j(\rho; z) = 0. \tag{11}$$

Since the operator in the left-hand side of equation (9) is self-adjoint, its eigenfunctions are orthonormal

$$\langle\hat{\Phi}_i(\rho; z)|\hat{\Phi}_j(\rho; z)\rangle_\rho = \int_0^\infty \hat{\Phi}_i(\rho; z)\hat{\Phi}_j(\rho; z)\rho\,\mathrm{d}\rho = \delta_{ij}, \tag{12}$$

where δ_{ij} is the Kronecker symbol. Therefore, we transform the solution of the above problem into the solution of an eigenvalue problem for a set of $j_{\max}$ ordinary second-order differential equations that determines the energy ϵ and the coefficients $\hat{\chi}^{(i)}(z)$ of expansion (8)

$$\left(-\mathbf{I}\frac{\mathrm{d}^2}{\mathrm{d}z^2} + \hat{\mathbf{U}}(z) + \hat{\mathbf{Q}}(z)\frac{\mathrm{d}}{\mathrm{d}z} + \frac{\mathrm{d}\hat{\mathbf{Q}}(z)}{\mathrm{d}z}\right)\hat{\chi}^{(i)}(z) = \epsilon_i\mathbf{I}\hat{\chi}^{(i)}(z). \tag{13}$$

Here $\mathbf{I}$, $\hat{\mathbf{U}}(z) = \hat{\mathbf{U}}(-z)$ and $\hat{\mathbf{Q}}(z) = -\hat{\mathbf{Q}}(-z)$ are the $j_{\max} \times j_{\max}$ matrices whose elements are expressed as

$$\begin{aligned}
\hat{U}_{ij}(z) &= \frac{\hat{E}_i(z) + \hat{E}_j(z)}{2}\delta_{ij} + \hat{H}_{ij}(z), \qquad I_{ij} = \delta_{ij}, \\
\hat{H}_{ij}(z) &= \hat{H}_{ji}(z) = \int_0^\infty \frac{\partial\hat{\Phi}_i(\rho; z)}{\partial z}\frac{\partial\hat{\Phi}_j(\rho; z)}{\partial z}\rho\,\mathrm{d}\rho, \\
\hat{Q}_{ij}(z) &= -\hat{Q}_{ji}(z) = -\int_0^\infty \hat{\Phi}_i(\rho; z)\frac{\partial\hat{\Phi}_j(\rho; z)}{\partial z}\rho\,\mathrm{d}\rho.
\end{aligned} \tag{14}$$

The discrete spectrum solutions obey the asymptotic boundary condition and the orthonormality conditions

$$\lim_{z\to\pm\infty} \hat{\chi}^{(i)}(z) = 0 \quad \rightarrow \quad \hat{\chi}^{(i)}(\pm z_{\max}) = 0, \qquad \int_{-z_{\max}}^{z_{\max}} (\hat{\chi}^{(i)}(z))^T\hat{\chi}^{(j)}(z)\,\mathrm{d}z = \delta_{ij}. \tag{15}$$

The application of this approach to the calculation of low-excited bound states of the hydrogen atom for $\gamma > 1$ and $-m = 0, \ldots, 10$ will be presented in the forthcoming paper [26] for $j_{\max} \sim 10$, while the cases of laboratory fields of $\gamma \sim 6$ T and $-m < 150$ were considered in [27].

2.2. Galerkin expansion

Consider a formal expansion of the partial solution $\Psi_i^{Em\sigma}(\rho, z)$ of equations (2)–(5) corresponding to the eigenstate $|m\sigma i\rangle$, in terms of the finite set of one-dimensional basis functions $\left\{\tilde{\Phi}_j^m(\rho)\right\}_{j=1}^{j_{\max}}$

$$\Psi_i^{Em\sigma}(\rho, z) = \sum_{j=1}^{j_{\max}} \tilde{\Phi}_j^m(\rho)\tilde{\chi}_j^{(m\sigma i)}(E, z). \tag{16}$$

In the Galerkin approach the wavefunctions $\tilde{\Phi}_j(\rho) = \tilde{\Phi}^m_j(\rho)$ and the potential curves $\tilde{E}_j$ (in Ry) are determined as the solutions of the following one-dimensional eigenvalue problem

$$\hat{A}_c \tilde{\Phi}_j(\rho) = \tilde{E}_j \tilde{\Phi}_j(\rho), \tag{17}$$

with the boundary conditions

$$\lim_{\rho\to 0} \rho \frac{\partial \tilde{\Phi}_j(\rho)}{\partial \rho} = 0, \qquad \text{for} \quad m = 0, \qquad \text{and} \qquad \tilde{\Phi}_j(0) = 0, \quad \text{for} \quad m \neq 0, \tag{18}$$

$$\lim_{\rho\to\infty} \tilde{\Phi}_j(\rho) = 0. \tag{19}$$

The above eigenvalue problem has the exact solution at fixed m, normalized like (12)

$$\begin{aligned} \tilde{\Phi}_j(\rho) &= \sqrt{\frac{\gamma N_\rho!}{(N_\rho + |m|)!}} \exp\left(-\frac{\gamma\rho^2}{4}\right) \left(\frac{\gamma\rho^2}{2}\right)^{\frac{|m|}{2}} L^{|m|}_{N_\rho}\left(\frac{\gamma\rho^2}{2}\right), \\ \tilde{E}_j &= \gamma(2N_\rho + |m| + m + 1), \end{aligned} \tag{20}$$

where $N_\rho = j - 1$ is the transversal quantum number and $L^{|m|}_{N_\rho}(x)$ is the associated Laguerre polynomial [20]. Note that the Galerkin expansion follows from the Kantorovich expansion at $z \to \pm\infty$, i.e.,

$$\tilde{\Phi}_j(\rho) = \lim_{z\to\pm\infty} \hat{\Phi}_j(\rho; z), \ \lim_{z\to\pm\infty} \hat{E}_j(z) = \tilde{E}_j = \epsilon^{\text{th}}_{mj}(\gamma) = \gamma(2N_\rho + |m| + m + 1). \tag{21}$$

Therefore, we transform the solution of the above problem into the solution of an eigenvalue problem for a set of $j_{\max}$ ordinary second-order differential equations that determines the energy ϵ and the coefficients $\tilde{\chi}^{(i)}(z)$ of expansion (16)

$$\left(-\mathbf{I}\frac{\mathrm{d}^2}{\mathrm{d}z^2} + \tilde{\mathbf{U}}(z)\right) \tilde{\chi}^{(i)}(z) = \epsilon_i \mathbf{I} \tilde{\chi}^{(i)}(z), \tag{22}$$

and the matrix $\tilde{\mathbf{U}}(z) = \tilde{\mathbf{U}}(-z)$ is expressed as

$$\tilde{U}_{ij}(z) = \frac{\tilde{E}_i + \tilde{E}_j}{2}\delta_{ij} - \int_0^\infty \tilde{\Phi}_i(\rho) \frac{2Z}{\sqrt{\rho^2 + z^2}} \tilde{\Phi}_j(\rho) \rho \, \mathrm{d}\rho. \tag{23}$$

The discrete spectrum solutions obey the asymptotic boundary condition and the orthonormality condition

$$\lim_{z\to\pm\infty} \tilde{\chi}^{(i)}(z) = 0 \quad \to \quad \tilde{\chi}^{(i)}(\pm z_{\max}) = 0, \qquad \int_{-z_{\max}}^{z_{\max}} (\tilde{\chi}^{(i)}(z))^T \tilde{\chi}^{(j)}(z) \, \mathrm{d}z = \delta_{ij}. \tag{24}$$

The application of this approach to the calculation of bound states of the hydrogen atom for $\gamma > 1$ is well known in [28]. The calculation of photoionizations of hydrogen in a strong magnetic field of $B \sim 600$–2000 T was considered within the frameworks of the multichannel quantum defect theory [29], while for the cases of laboratory fields of $B \sim 6$ T such a type of calculations is of course not practicable, because $j_{\max} \sim 200$.

2.3. Relation between the parity functions and the functions having physical scattering asymptotic form in cylindrical coordinates

The asymptotic form of the coefficients $\tilde{\chi}^{(n)}(z)$ of expansion (16) (or $\hat{\chi}^{(n)}(z)$ of expansion (8)) with fixed m, σ and $\epsilon = 2E$ for the nth solution in open channels is

$$\chi_{Em\sigma n'n}(z \to \pm\infty) = \begin{cases} \dfrac{a_{+1n'n}}{\sqrt{p_{n'}}} \cos\left(p_{n'}z + \dfrac{Z}{p_{n'}}\dfrac{z}{|z|}\ln(2p_{n'}|z|) + \dfrac{z}{|z|}\delta_{+1n}\right), & \sigma = +1, \\ \dfrac{a_{-1n'n}}{\sqrt{p_{n'}}} \sin\left(p_{n'}z + \dfrac{Z}{p_{n'}}\dfrac{z}{|z|}\ln(2p_{n'}|z|) + \dfrac{z}{|z|}\delta_{-1n}\right), & \sigma = -1, \end{cases} \tag{25}$$

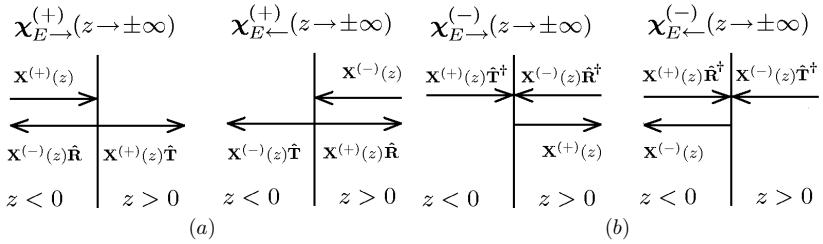

Figure 2. Schematic diagrams of the continuum spectrum states' waves having the asymptotic form: (*a*) 'incident wave + outgoing wave', (*b*) 'incident wave + ingoing wave'.

where $p_n = \sqrt{2E - \epsilon^{\rm th}_{mn}} \geqslant 0$ and $n, n' = 1, \ldots, N_o$, $\delta_{\sigma n} = \delta^{\sigma}_n + \delta^c_n - (\sigma+1)\pi/4$ are the phase shifts, δ^{σ}_n and δ^c_n are the eigenchannel short-range and Coulomb phase shifts, $a_{\sigma n' n} = C^{\sigma}_{n' n}$ are the amplitudes or mixed parameters defined in section 4 and $N_o = \max_{2E \geqslant \epsilon^{\rm th}_{mn}} n$ is the number of open channels. Equation (25) may be rewritten in the matrix form, so that

$$\chi_{E\sigma}(z \rightarrow \pm\infty) = \begin{cases} \begin{cases} \frac{1}{2}\mathbf{X}^{(+)}(z)\mathbf{A}_{+1} + \frac{1}{2}\mathbf{X}^{(-)}(z)\mathbf{A}^*_{+1}, & \sigma = +1, \\ \frac{1}{2\imath}\mathbf{X}^{(+)}(z)\mathbf{A}_{-1} - \frac{1}{2\imath}\mathbf{X}^{(-)}(z)\mathbf{A}^*_{-1}, & \sigma = -1, \end{cases} & z > 0, \\ \begin{cases} \frac{1}{2}\mathbf{X}^{(+)}(z)\mathbf{A}^*_{+1} + \frac{1}{2}\mathbf{X}^{(-)}(z)\mathbf{A}_{+1}, & \sigma = +1, \\ \frac{1}{2\imath}\mathbf{X}^{(+)}(z)\mathbf{A}^*_{-1} - \frac{1}{2\imath}\mathbf{X}^{(-)}(z)\mathbf{A}_{-1}, & \sigma = -1, \end{cases} & z < 0, \end{cases} \tag{26}$$

where coefficients of matrices $\mathbf{X}^{(\pm)}(z)$ and $\mathbf{A}_{\pm 1}$ take the form

$$X^{(\pm)}_{n' n}(z) = p^{-1/2}_{n'} \exp\left(\pm\imath p_{n'} z \pm \imath \frac{Z}{p_{n'}} \frac{z}{|z|} \ln(2p_{n'}|z|)\right) \delta_{n' n}, \tag{27}$$

$$A_{\sigma n' n} = a_{\sigma n' n} \exp(\imath \delta_{\sigma n}). \tag{28}$$

On the other hand, the function that describes the incidence of the particle and its scattering, having the asymptotic form 'incident wave + outgoing wave' (see figure 2(*a*)), is

$$\chi^{(+)}_{E\hat{v}}(z \rightarrow \pm\infty) = \begin{cases} \begin{cases} \mathbf{X}^{(+)}(z)\hat{\mathbf{T}}, & z > 0, \\ \mathbf{X}^{(+)}(z) + \mathbf{X}^{(-)}(z)\hat{\mathbf{R}}, & z < 0, \end{cases} & \hat{v} = \rightarrow, \\ \begin{cases} \mathbf{X}^{(-)}(z) + \mathbf{X}^{(+)}(z)\hat{\mathbf{R}}, & z > 0, \\ \mathbf{X}^{(-)}(z)\hat{\mathbf{T}}, & z < 0, \end{cases} & \hat{v} = \leftarrow, \end{cases} \tag{29}$$

where $\hat{\mathbf{T}}$ and $\hat{\mathbf{R}}$ are the transmission and reflection amplitude matrices, $\hat{\mathbf{T}}^{\dagger}\hat{\mathbf{T}} + \hat{\mathbf{R}}^{\dagger}\hat{\mathbf{R}} = \mathbf{I}_{oo}$, $\hat{v}$ denotes the initial direction of the particle motion along the z axis and $\mathbf{I}_{oo}$ is the unit $N_o \times N_o$ matrix. Note that due to the symmetry of the scattering potential the transmission and reflection coefficients are independent of the direction of the incident wave vector.

This wavefunction may be presented as a linear combination of the solutions having positive and negative parities:

$$\chi^{(+)}_{E\overrightarrow{\leftarrow}}(z) = \chi_{E,+1}(z)\mathbf{B}_{+1} \pm \imath \chi_{E,-1}(z)\mathbf{B}_{-1}. \tag{30}$$

It is easy to show that $\mathbf{B}_{\sigma} = [\mathbf{A}^*_{\sigma}]^{-1}$, and $\hat{\mathbf{T}}$ and $\hat{\mathbf{R}}$ are defined by

$$\begin{aligned} \hat{\mathbf{T}} &= \tfrac{1}{2}(\mathbf{A}_{+1}\mathbf{B}_{+1} + \mathbf{A}_{-1}\mathbf{B}_{-1}) = \tfrac{1}{2}(-\check{\mathbf{S}}_{+1} + \check{\mathbf{S}}_{-1}), \\ \hat{\mathbf{R}} &= \tfrac{1}{2}(\mathbf{A}_{+1}\mathbf{B}_{+1} - \mathbf{A}_{-1}\mathbf{B}_{-1}) = \tfrac{1}{2}(-\check{\mathbf{S}}_{+1} - \check{\mathbf{S}}_{-1}), \end{aligned} \tag{31}$$

where $\check{\mathbf{S}}_\sigma$ is the scattering matrix at fixed σ defined by (28). However, to calculate the ionization cross section it is necessary to use the function having the reverse asymptotic form 'incident wave + ingoing wave' (see figure 2(*b*)), that is

$$\chi^{(-)}_{E\hat{v}}(z\to\pm\infty)=\begin{cases}\begin{cases}\mathbf{X}^{(+)}(z)+\mathbf{X}^{(-)}(z)\hat{\mathbf{R}}^\dagger, & z>0,\\ \mathbf{X}^{(+)}(z)\hat{\mathbf{T}}^\dagger, & z<0,\end{cases}, & \hat{v}=\rightarrow,\\ \begin{cases}\mathbf{X}^{(-)}(z)\hat{\mathbf{T}}^\dagger, & z>0,\\ \mathbf{X}^{(-)}(z)+\mathbf{X}^{(+)}(z)\hat{\mathbf{R}}^\dagger, & z<0,\end{cases}, & \hat{v}=\leftarrow,\end{cases} \tag{32}$$

or

$$\chi^{(-)}_{E\overrightarrow{\leftarrow}}(z)=\chi_{E,+1}(z)\mathbf{B}^*_{+1}\pm\imath\chi_{E,-1}(z)\mathbf{B}^*_{-1}. \tag{33}$$

Note that $\left(\chi^{(-)}_{E\overrightarrow{\leftarrow}}(z)\right)^*=\chi^{(+)}_{E\overleftarrow{\rightarrow}}(z)$. The functions are normalized so that

$$\sum_{n''=1}^{j_{\max}}\int_{-\infty}^{\infty}\left(\chi^{(\pm)}_{E'm\hat{v}'n''n'}(z)\right)^*\chi^{(\pm)}_{Em\hat{v}n''n}(z)\,\mathrm{d}z=2\pi\delta(E'-E)\delta_{\hat{v}'\hat{v}}\delta_{n'n}. \tag{34}$$

The $\hat{\mathbf{S}}$-matrix may be composed of the transmission and reflection amplitudes

$$\hat{\mathbf{S}}=\begin{pmatrix}\hat{\mathbf{T}} & \hat{\mathbf{R}}\\ \hat{\mathbf{R}} & \hat{\mathbf{T}}\end{pmatrix}. \tag{35}$$

This matrix is unitary, since $\hat{\mathbf{T}}^\dagger\hat{\mathbf{T}}+\hat{\mathbf{R}}^\dagger\hat{\mathbf{R}}=\mathbf{I}_{oo}$ and $\hat{\mathbf{R}}^\dagger\hat{\mathbf{T}}+\hat{\mathbf{T}}^\dagger\hat{\mathbf{R}}=\mathbf{0}$. These conditions will be used to check the accuracy of numerical multichannel calculations of continuous spectrum wavefunctions in section 5.

To calculate the ionization it is convenient to use the function renormalized to $\delta(E'-E)$, i.e., divided by $\sqrt{2\pi}$:

$$|E\hat{v}mN_\rho\rangle=\frac{\exp(\imath m\varphi)}{2\pi}\sum_{n'=1}^{j_{\max}}\tilde{\Phi}_{n'}(\rho)\tilde{\chi}^{(-)}_{Em\hat{v}n'n}(z) \tag{36}$$

or

$$|E\hat{v}mN_\rho\rangle=\frac{\exp(\imath m\varphi)}{2\pi}\sum_{n'=1}^{j_{\max}}\hat{\Phi}_{n'}(\rho;z)\hat{\chi}^{(-)}_{Em\hat{v}n'n}(z), \tag{37}$$

where $N_\rho=n-1$. The expression for the cross section of ionization by the light linearly polarized along the axis z is

$$\sigma^d_{Nlm}(\omega)=4\pi^2\alpha\omega\sum_{N_\rho=0}^{N_\rho-1}\sum_{\hat{v}}|\langle E\hat{v}mN_\rho|z|Nlm\rangle|^2a_0^2. \tag{38}$$

In the above expressions $\omega=E-E_{Nlm}$ is the frequency of radiation, E_{Nlm} is the energy of the initial bound state $|Nlm\rangle$ specified by the spherical quantum numbers N,l,m defined in section 3, α is the fine-structure constant, a_0 is the Bohr radius.

For recombination the wavefunction should be renormalized to one particle per unit length in the incident wave

$$|vmN_\rho\rangle=\sqrt{p_n}\frac{\exp(\imath m\varphi)}{\sqrt{2\pi}}\sum_{n'=1}^{j_{\max}}\tilde{\Phi}_{n'}(\rho)\tilde{\chi}^{(+)}_{Em\hat{v}n'n}(z) \tag{39}$$

or

$$|vmN_\rho\rangle=\sqrt{p_n}\frac{\exp(\imath m\varphi)}{\sqrt{2\pi}}\sum_{n'=1}^{j_{\max}}\hat{\Phi}_{n'}(\rho;z)\hat{\chi}^{(+)}_{Em\hat{v}n'n}(z), \tag{40}$$

where $v = \hat{v}p_n$ and $N_\rho = n - 1$. The expression for the rate of recombination induced by the light linearly polarized along the axis z for the particle, initially moving in the channel N_ρ with the velocity v has the form

$$\lambda^{rec}_{NN_\rho}(v) = 4\pi^2\alpha I \sum_{l=0}^{N-1}\sum_{m=-l}^{0} |\langle Nlm|z|vmN_\rho\rangle|^2\delta(E - E_{Nlm} - \omega)a_0^2, \tag{41}$$

I being the intensity of the incident light.

For the light circularly polarized in the plane xOy the above expressions read as

$$\sigma^p_{Nlm}(\omega) = 4\pi^2\alpha\omega \sum_{N_\rho=0}^{N_o-1}\sum_{\hat{v}} |\langle E\hat{v}m \pm 1N_\rho|\vec{e}_\pm\vec{r}|Nlm\rangle|^2 a_0^2, \tag{42}$$

$$\lambda^{rec}_{NN_\rho}(v) = 4\pi^2\alpha I \sum_{l=0}^{N-1}\sum_{m=-l}^{0} |\langle Nlm \pm 1|\vec{e}_\pm\vec{r}|vmN_\rho\rangle|^2\delta(E - E_{Nlm} - \omega)a_0^2, \tag{43}$$

where the complex unit vectors are $\vec{e}_\pm = \frac{1}{\sqrt{2}}\vec{i} \pm \frac{\imath}{\sqrt{2}}\vec{j}$.

3. Statement of the problem in spherical coordinates

In the spherical coordinates (r, θ, φ) (see figure 1) equation (2) can be rewritten as [31]

$$\left(-\frac{1}{r^2}\frac{\partial}{\partial r}r^2\frac{\partial}{\partial r} + \frac{1}{r^2}\hat{A}(p) - \frac{2Z}{r}\right)\Psi(r,\eta) = \epsilon\Psi(r,\eta) \tag{44}$$

in the domain Ω: $0 < r < \infty$ and $-1 < \eta = \cos\theta < 1$. Here $\hat{A}(p)$ is the parametric Hamiltonian

$$\hat{A}(p) = -\frac{\partial}{\partial\eta}(1-\eta^2)\frac{\partial}{\partial\eta} + \frac{m^2}{1-\eta^2} + 2pm + p^2(1-\eta^2), \tag{45}$$

$p = \gamma r^2/2$ and $\Psi(r,\eta) \equiv \Psi^{m\sigma}(r,\eta) = \sigma\Psi^{m\sigma}(r,-\eta)$. The sign of z-parity $\sigma = (-1)^{N_\eta}$ is defined by the number of nodes N_η of the solution $\Psi(r,\eta)$ as a function of η. We will also use the scaled radial variable $\hat{r} = r\sqrt{\gamma}$, the effective charge $\hat{Z} = Z/\sqrt{\gamma}$ and the scaled energy $\hat{\epsilon} = \epsilon/\gamma$ or $\hat{E} = E/\gamma$. Practically it means replacing γ with 1 and multiplying Z by $1/\sqrt{\gamma}$ and ϵ or E by $1/\gamma$ in all equations above.

The boundary conditions in each $m\sigma$ subspace of the full Hilbert space have the form

$$\lim_{\eta\to\pm1}(1-\eta^2)\frac{\partial\Psi(r,\eta)}{\partial\eta} = 0, \qquad \text{for} \quad m = 0, \quad \text{and} \quad \Psi(r,\pm1) = 0, \qquad \text{for} \quad m \neq 0, \tag{46}$$

$$\lim_{r\to0} r^2\frac{\partial\Psi(r,\eta)}{\partial r} = 0. \tag{47}$$

The wavefunction of the discrete spectrum obeys the asymptotic boundary condition. Approximately this condition is replaced by the boundary condition of the first type at large, but finite $r = r_{\max}$, namely,

$$\lim_{r\to\infty} r^2\Psi(r,\eta) = 0 \quad \to \quad \Psi(r_{\max},\eta) = 0. \tag{48}$$

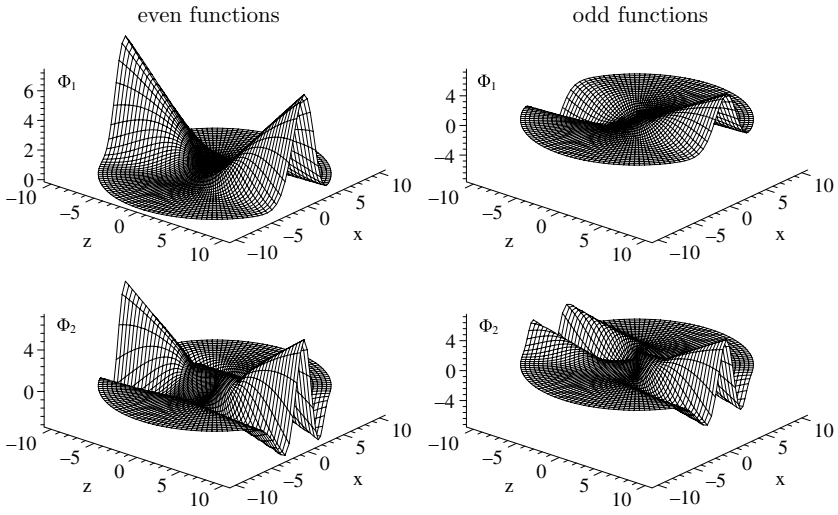

Figure 3. Profiles of the even $\Phi_i \equiv \Phi^{m\sigma=+1}(\eta; r)$ and odd $\Phi_i \equiv \Phi^{m\sigma=-1}(\eta; r)$ basis functions at $m = 0$ and $\gamma = 1$ for $i = 1, 2$ in the zx plane.

In the Fano-Lee **R**-matrix theory [14, 15] the wavefunction of the continuum $\Psi(r, \eta)$ obeys the boundary condition of the third type at fixed values of the energy ϵ and the radial variable $r = r_{\max}$

$$\frac{\partial \Psi(r, \eta)}{\partial r} - \mu \Psi(r, \eta) = 0. \tag{49}$$

Here the parameters $\mu \equiv \mu(r_{\max}, \epsilon)$, determined by the variational principle, play the role of eigenvalues of the logarithmic normal derivative matrix of the solution of the boundary problem (44)–(47) and (49).

3.1. Kantorovich expansion

Consider a formal expansion of the partial solution $\Psi_i^{Em\sigma}(r, \eta)$ of equations (44)–(47) with conditions (48) and (49), corresponding to the eigenstate $|m\sigma i\rangle$, in terms of the finite set of one-dimensional basis functions $\{\Phi_j^{m\sigma}(\eta; r)\}_{j=1}^{j_{\max}}$

$$\Psi_i^{Em\sigma}(r, \eta) = \sum_{j=1}^{j_{\max}} \Phi_j^{m\sigma}(\eta; r) \chi_j^{(m\sigma i)}(E, r). \tag{50}$$

In equation (50) the functions $\chi^{(i)}(r) \equiv \chi^{(m\sigma i)}(E, r)$, $(\chi^{(i)}(r))^T = (\chi_1^{(i)}(r), \ldots, \chi_{j_{\max}}^{(i)}(r))$ are unknown and the surface functions $\mathbf{\Phi}(\eta; r) \equiv \mathbf{\Phi}^{m\sigma}(\eta; r) = \sigma \mathbf{\Phi}^{m\sigma}(-\eta; r)$, $(\mathbf{\Phi}(\eta; r))^T = (\Phi_1(\eta; r), \ldots, \Phi_{j_{\max}}(\eta; r))$ form an orthonormal basis for each value of r which is treated as a parameter (see figure 3).

In the Kantorovich approach the wavefunctions $\Phi_j(\eta; r)$ and the potential curves $E_j(r)$ (in Ry) are determined as the solutions of the following one-dimensional parametric eigenvalue problem

$$\hat{A}(p)\Phi_j(\eta; r) = E_j(r)\Phi_j(\eta; r), \tag{51}$$

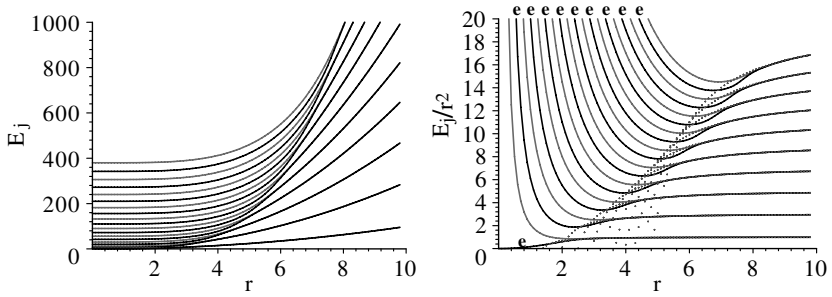

Figure 4. Potential curves $E_j(r)$, $j = 1, 2, \ldots$ at $m = 0$ and $\gamma = 1$ for some first even $j = (l - |m|)/2 + 1$ (marked by 'e') and odd $j = (l - |m| + 1)/2$ states. Dotted lines display the asymptotic behavior at large r.

with the boundary conditions

$$\lim_{\eta\to\pm1}(1-\eta^2)\frac{\partial\Phi_j(\eta;r)}{\partial\eta} = 0, \quad \text{for} \quad m = 0 \quad \text{and} \quad \Phi_j(\pm1;r) = 0, \quad \text{for} \quad m \neq 0. \tag{52}$$

Since the operator in the left-hand side of equation (51) is self-adjoint, its eigenfunctions are orthonormal,

$$\langle\Phi_i(\eta;r)|\Phi_j(\eta;r)\rangle_\eta = \int_{-1}^{1}\Phi_i(\eta;r)\Phi_j(\eta;r)\,\mathrm{d}\eta = \delta_{ij}. \tag{53}$$

Note that the solutions of this problem with shifted eigenvalues, $\check{E}_j(r) = E_j(r) - 2pm$, correspond to the solutions of the eigenvalue problem for the AOSF [20]

$$A(p)\Phi_j(\eta;r) = \check{E}_j(r)\Phi_j(\eta;r), \tag{54}$$

where $A(p) = \hat{A}(p) - 2pm$. At fixed values $\sigma = \pm1$ and $|m|$ the eigenfunctions $\Phi_j(\theta;r)$ are sought in the form of a series expansion over the normalized associated Legendre polynomials $P^{|m|}_{|m|+s}(\eta)$ [20] with unknown coefficients $c^{|m|\sigma}_{sj}(r)$,

$$\Phi_j(\eta;r) = \sum_{s=(1-\sigma)/2}^{s_{\max}} c^{|m|\sigma}_{sj}(r)\,P^{|m|}_{|m|+s}(\eta), \tag{55}$$

where s is an even (odd) integer at $\sigma = (-1)^s = \pm1$. The calculations of eigenfunctions $\Phi_j(\theta;r)$ and of eigenvalues $E_i(r)$ were performed by a special choice of value $s_{\max}$ to achieve a relative computer accuracy using the code POTHMF realizing in FORTRAN [23]. Their plots are presented in figures 3 and 4. For small p the asymptotic behavior of the eigenvalues $E_j(r)$, $j = 1, 2, \ldots$ at fixed values of m and σ is determined by the values of the orbital quantum number l labeled by a conventional sequences of $\{s, p, d, f, g, h, i, k, l, \ldots\}$: $E_j(0) = l(l+1)$, $l = 0, 1, \ldots$, where $j = (l-|m|)/2+1$ for even states, $\sigma = +1 = (-1)^{l-|m|}$ and $j = (l - |m| + 1)/2$ for odd states, $\sigma = -1 = (-1)^{l-|m|}$, defined by $\Phi_j(\eta;0) = P^{|m|}_l(\eta)$. Taking into account the fact that the number of nodes N_η of the eigenfunction $\Phi_j(\eta;r)$ at fixed m and $\sigma = (-1)^{N_\eta}$ does not depend on the parameter p, we find a one-to-one correspondence between these sets, i.e., $N_\eta = l - |m|$.

For large r the asymptotic behavior of the eigenfunctions $\Phi_j(\eta;r)$ and eigenvalues $E_j(r)$ at fixed values of m and σ is determined by the value of the transversal quantum number,

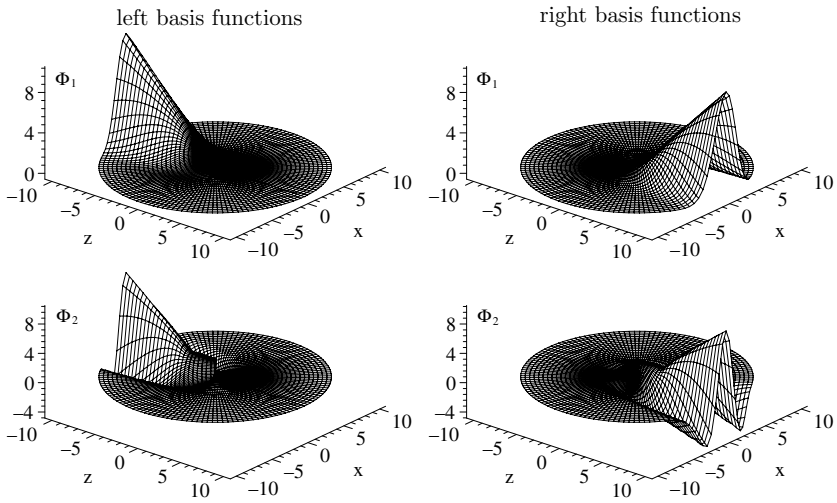

Figure 5. Profiles of the left $\Phi_i \equiv \Phi^{m\rightarrow}(\eta; r)$ and right $\Phi_i \equiv \Phi^{m\leftarrow}(\eta; r)$ basis functions at $m = 0$ and $\gamma = 1$ for $i = 1, 2$ in the zx plane.

$N_\rho = j - 1$ (see equations (20) and (21) and section 3.4)

$$\begin{aligned} &\tilde{\Phi}_j(\rho) = \lim_{r\to\infty, |\eta|\sim 1} r^{-1}\Phi_j(|\eta|; r), \\ &\lim_{r\to\infty} r^{-2}E_j(r) = \epsilon^{\text{th}}_{mj}(\gamma) = \gamma(2N_\rho + |m| + m + 1). \end{aligned} \tag{56}$$

The transversal quantum number N_ρ, i.e., the number of nodes of the eigenfunction $\mathbf{\Phi}^{m\sigma}(\eta; r)$ in the subinterval $0 < \eta < 1$ or $-1 < \eta < 0$, can be expressed via N_η as follows: $N_\rho = N_\eta/2$ for the even states, $\sigma = +1$ and $N_\rho = (N_\eta - 1)/2$ for the odd states, $\sigma = -1$. It means that the eigenfunctions

$$\mathbf{\Phi}^{m\hat{v}}(\eta; r) = \frac{\mathbf{\Phi}^{m\sigma=+1}(\eta; r) \pm \mathbf{\Phi}^{m\sigma=-1}(\eta; r)}{\sqrt{2}}, \tag{57}$$

labeled by $\hat{v} = \overleftarrow{\rightarrow}$ at large r are localized in the vicinity of $\eta = \pm 1$ (i.e., at $z \to +\infty$ and $z \to -\infty$) and have N_ρ nodes in the subintervals $0 < \eta < 1$ and $-1 < \eta < 0$, respectively (see figure 5). Such asymptotic functions $\mathbf{\Phi}^{m\hat{v}}(\eta; r)$ correspond to $\tilde{\mathbf{\Phi}}^m(\rho)$ in equations (20) and (21). Their asymptotic behavior is considered in section 3.4. Taking into account the above-mentioned correspondence rules between the quantum numbers N_η and N_ρ and number j at fixed values m and σ, we will use the unified number, j, without pointing out explicitly a concrete type of quantum numbers.

From here on we transform the solution of problem (44) into the solution of an eigenvalue problem for a set of $j_{\max}$ ordinary second-order differential equations that determine the energy ϵ and the coefficients $\boldsymbol{\chi}^{(i)}(r)$ of expansion (50) (the radial wavefunctions):

$$\left(-\mathbf{I}\frac{1}{r^2}\frac{\mathrm{d}}{\mathrm{d}r}r^2\frac{\mathrm{d}}{\mathrm{d}r} + \frac{\mathbf{U}(r)}{r^2} + \mathbf{Q}(r)\frac{\mathrm{d}}{\mathrm{d}r} + \frac{1}{r^2}\frac{\mathrm{d}r^2\mathbf{Q}(r)}{\mathrm{d}r}\right)\boldsymbol{\chi}^{(i)}(r) = \epsilon_i\mathbf{I}\boldsymbol{\chi}^{(i)}(r), \tag{58}$$

$$\lim_{r\to 0} r^2\left(\frac{\mathrm{d}\boldsymbol{\chi}^{(i)}(r)}{\mathrm{d}r} - \mathbf{Q}(r)\boldsymbol{\chi}^{(i)}(r)\right) = 0. \tag{59}$$

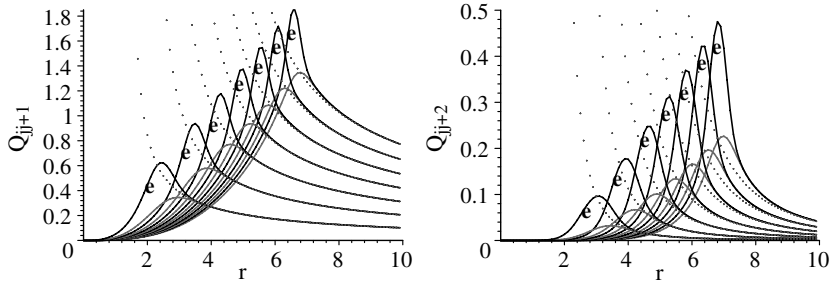

Figure 6. Radial matrix elements $Q_{ij}(r)$ for even (marked by 'e') and odd parities at $m = 0$ and $\gamma = 1$. Dotted lines display the asymptotic behavior at large r.

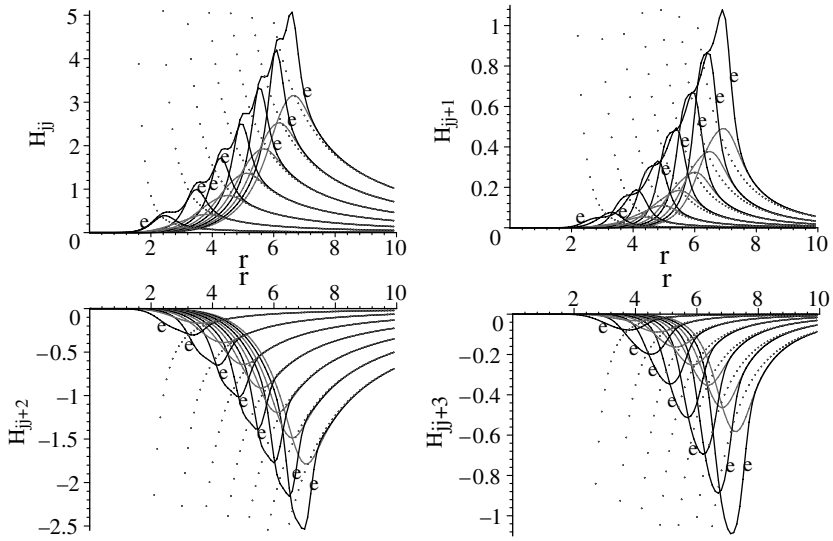

Figure 7. Radial matrix elements $H_{ij}(r)$ for even (marked by 'e') and odd parities at $m = 0$ and $\gamma = 1$. Dotted lines display the asymptotic behavior at large r.

Here $\mathbf{U}(r)$ and $\mathbf{Q}(r)$ are $j_{\max} \times j_{\max}$ matrices with the elements expressed as

$$
\begin{aligned}
U_{ij}(r) &= \frac{E_i(r) + E_j(r)}{2}\delta_{ij} - 2Zr\delta_{ij} + r^2 H_{ij}(r), \\
H_{ij}(r) &= H_{ji}(r) = \int_{-1}^{1} \frac{\partial \Phi_i(\eta; r)}{\partial r} \frac{\partial \Phi_j(\eta; r)}{\partial r}\, \mathrm{d}\eta, \\
Q_{ij}(r) &= -Q_{ji}(r) = -\int_{-1}^{1} \Phi_i(\eta; r) \frac{\partial \Phi_j(\eta; r)}{\partial r}\, \mathrm{d}\eta.
\end{aligned}
\tag{60}
$$

The calculations of radial coupling matrix elements $H_{ij}(r)$ and $Q_{ij}(r)$ were performed by a special choice of value of matching point r_{match} of their asymptotic form from section 3.4 to achieve a relative computer accuracy using the code POTHMF realizing in FORTRAN [23]. Their plots are presented in figures 6 and 7. The peculiarities of behavior of the plots and the corresponding asymptotics are considered in section 3.4.

The discrete spectrum solutions obey the asymptotic boundary condition and the orthonormality conditions

$$\lim_{r\to\infty} r^2\boldsymbol{\chi}^{(i)}(r) = 0 \quad \rightarrow \quad \boldsymbol{\chi}^{(i)}(r_{\max}) = 0, \qquad \int_0^{r_{\max}} r^2(\boldsymbol{\chi}^{(i)}(r))^T\boldsymbol{\chi}^{(j)}(r)\,\mathrm{d}r = \delta_{ij}. \tag{61}$$

The continuous spectrum solution $\boldsymbol{\chi}^{(i)}(r)$ satisfies the third-type boundary condition

$$\frac{\mathrm{d}\boldsymbol{\chi}(r)}{\mathrm{d}r} = \mathbf{R}\boldsymbol{\chi}(r), \qquad r = r_{\max}, \tag{62}$$

where the nonsymmetrical matrix $\mathbf{R}$ is calculated using the method of [21].

Thus, within the framework of the Kantorovich approach the original problem is reduced to the following steps.

- The calculation of the potential curves $E_j(r)$ and eigenfunctions $\Phi_j(\theta; r)$ of the spectral problem (51)–(53) for a given set of $r \in \omega_r$ at fixed values m and $\gamma = 1$.
- The calculation of the derivatives $\partial\boldsymbol{\Phi}(\theta; r)/\partial r$ and the corresponding integrals (see (60)) for the radial coupling matrices $\mathbf{U}(r)$ and $\mathbf{Q}(r)$.
- The calculation of the scaled energies $\hat{\epsilon}$ and radial wavefunctions $\boldsymbol{\chi}^{(i)}(r)$ as solutions of 1D-eigenvalue problem (58)–(60) with the conditions (61) at fixed m, $\gamma = 1$ and the effective charge $\hat{Z} = Z/\sqrt{\gamma}$. Analysis of the convergence of the solutions depending on the number of channels $j_{\max}$. Recalculation of the scaled energies into the initial ones $\epsilon = \hat{\epsilon}\gamma$ or $E = \hat{E}\gamma$.
- The calculation of the matrix $\mathbf{R}$ and the reaction matrix $\mathbf{K}$ (equations (62) and (100)), corresponding to the radial wavefunctions $\boldsymbol{\chi}^{(i)}(r)$, as solutions of 1D-eigenvalue problem (58)–(60) with the condition (62) at fixed m, $\gamma = 1$, the effective charge $\hat{Z} = Z/\sqrt{\gamma}$ and the scaled energy $\hat{\epsilon}$ or $\hat{E}$. The analysis of the convergence of the solutions depends on the number of channels $j_{\max}$.

Taking into account the above rules of correspondence and the asymptotic behavior of the eigenvalues $E_i(r)$ at large r (see also section 3.4), we can express the values of the binding energy $\mathcal{E}$ via the eigenvalues ϵ_i of the problem (58)–(61) numbered by a vibration quantum number, $v = 0, 1, 2, \ldots$, in ascending order $\epsilon_i = \epsilon_{iv}$: $\epsilon_{i0} < \epsilon_{i1} < \epsilon_{i2} < \cdots$, as $\mathcal{E} = \left(\epsilon^{\mathrm{th}}_{mi}(\gamma) - \epsilon_{iv}\right)/2$ (in au), where $\epsilon^{\mathrm{th}}_{m\sigma i}(\gamma)$ is the true threshold shift (56) or the reduced one $\epsilon^{\mathrm{th}}_{m}(\gamma) = \gamma(|m| + m + 1)$. Then for $\gamma \to 0$ one can mark eigenvalues $\epsilon_i = \epsilon_{iv}$ by a set of quantum numbers $(NN_rm\sigma)$, where N is a principal quantum number of a free-hydrogen-like atom and N_r is an integer that numerates in ascending order the zero-order degenerate perturbation theory energy, $\epsilon_{iv} = 2E^{(0)}_N + 2E^{(1)}_{NN_rm\sigma}\gamma^2 + O(\gamma^4)$ at fixed N. The corresponding zero-order approximation states, $|NN_rm\sigma\rangle$, are determined by a linear combination of free-hydrogen atom states $|Nlm\rangle$ and are labeled by $N_r = 0, 2, \ldots, 2[(N-1-|m|)/2]$ for $\sigma = +1$ and $N_r = 1, 3, \ldots, 2[(N-|m|)/2] - 1$ for $\sigma = -1$. The latter can be marked also by a set of spherical quantum numbers (Nlm) because of the correspondence of the number of radial nodes, $N_r = N - l - 1$, of the free-hydrogen states and the number of changing sign, $[N_r/2]$, of coefficients of the linear combination $|NN_rm\sigma\rangle$. To show this correspondence visually, we display in figures 8 and 9, as an example, a comparison of the three-dimensional plots of the normalized wavefunctions in the zx plane of the free-hydrogen atom spherical states $|Nlm\rangle$ and anisotropic zero-order approximation states $|NN_rm\sigma\rangle$ separated by parity $\sigma = \pm 1$ for a manifold with $N = 9$ and $m = 0$, for which the convergence of the method for

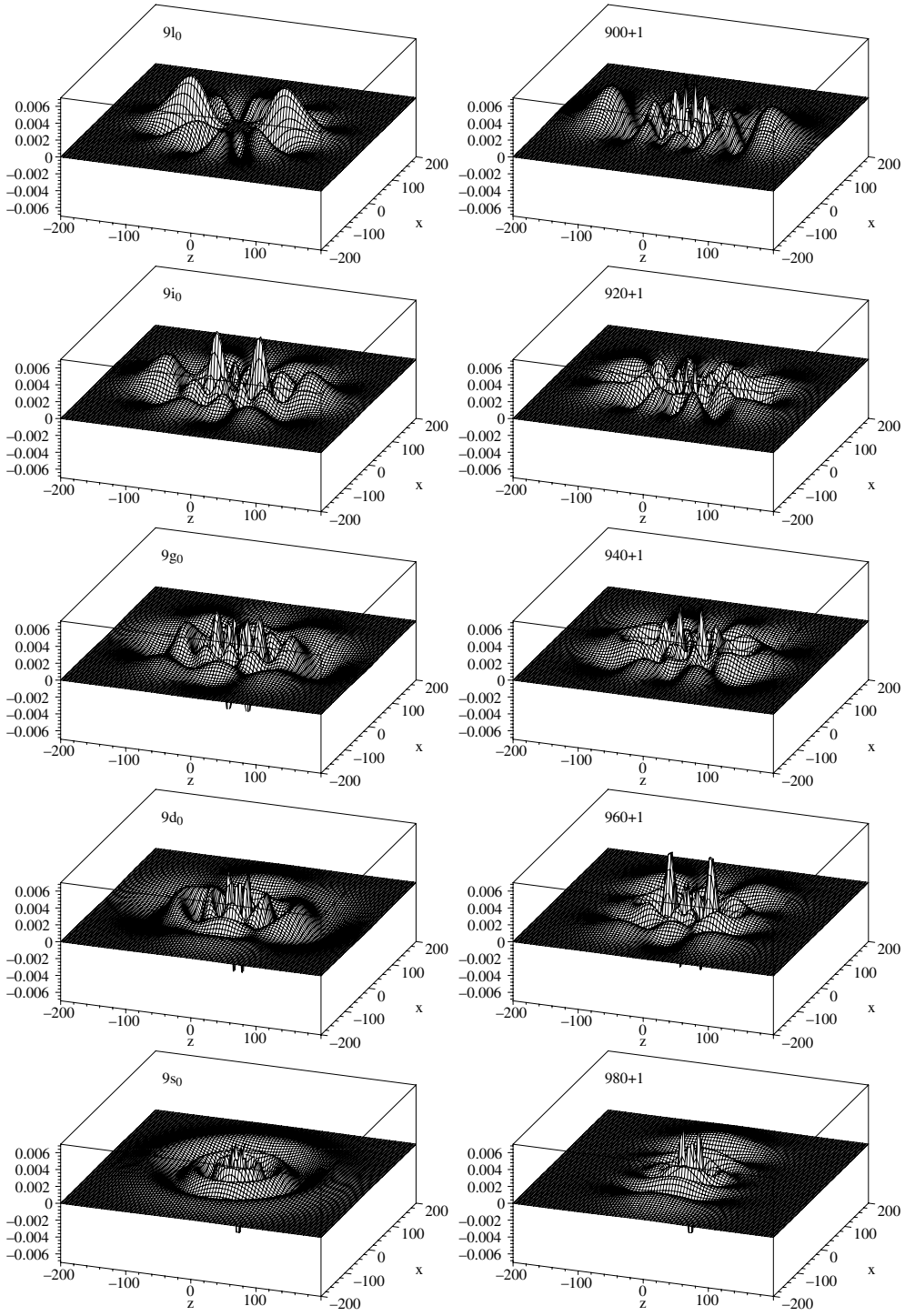

Figure 8. The three-dimensional plots of the normalized even wavefunctions ($\sigma = +1$) in the zx plane of free-hydrogen atom states $|Nlm\rangle$ and zero-order approximation states $|NN_rm\sigma\rangle$ for a manifold with $N = 9$ and $m = 0$.

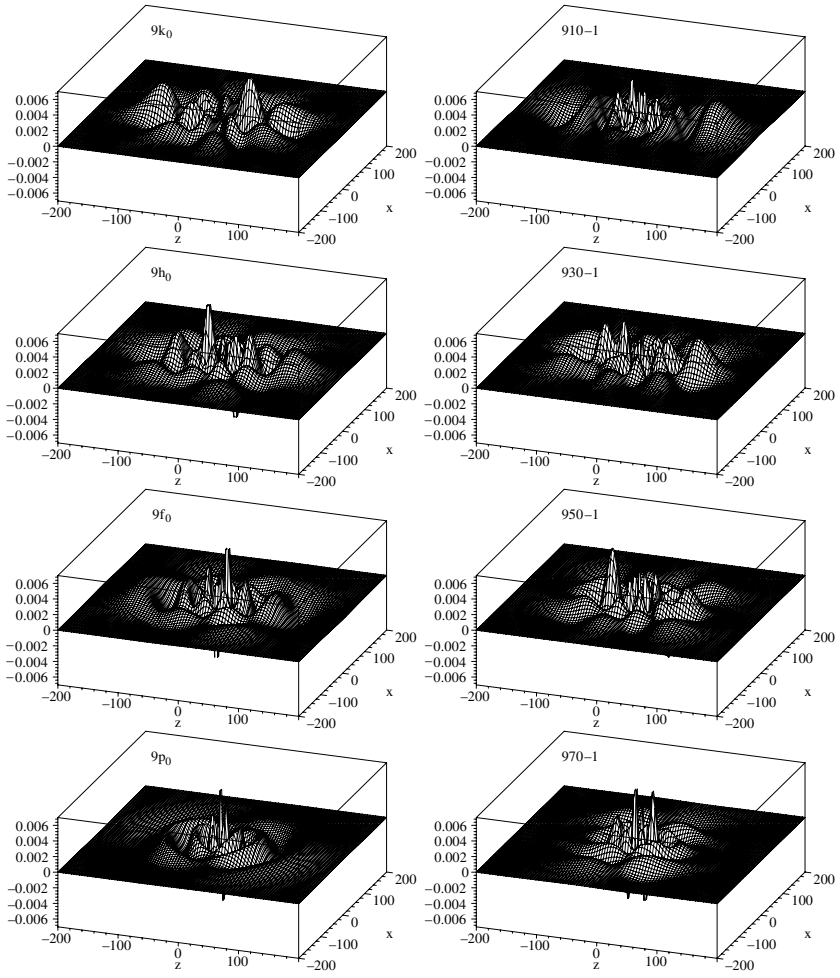

Figure 9. Same as in figure 8 but odd wavefunctions ($\sigma = -1$).

the energy of states by $j_{\max}$ has been studied in paper [9]. One can see that for anisotropic states belong to the lower part of the spectrum the so-called vibrational states (with minimum energy corrections $E^{(1)}_{NN_r m\sigma}$) are distributed mainly along the z-axis while for anisotropic states belong to the upper part of the spectrum the so-called rotational states (with maximum energy corrections $E^{(1)}_{NN_r m\sigma}$) are distributed mainly across the z-axis. An appearance of anisotropy of such states in the photoionization cross-section calculations will be shown explicitly in section 5. Indeed, for $\gamma \to 0$ it is sufficient to cut $j_{\max} \geqslant 2[(N - |m|)/2]$ in (58)–(61), while for $\gamma \to \infty$ a diagonal approximation of equations (16) and (8) or an effective approximation of equations (58)–(61) given in appendix B is sufficient to yield the known adiabatic classification by $[N_\rho N_z]$ or $[N_\rho N_{|z|}]$ with fixed m, σ. Here adiabatic quantum numbers $N_z = 2N_{|z|} + (1 - \sigma)/2$ and $N_{|z|}$ can be determined as a sum of the number of nodes, N_r, and the number of changing sign of coefficients of the linear combination $|NN_r m\sigma\rangle$, i.e. $N_{|z|} = [(N + 1 - |m| - (1 - \sigma)/2)/2][(N - |m| - (1 - \sigma)/2)/2] + [N_r/2]$.

3.2. Expansion of the matrix elements at small r

In accordance with [22] the asymptotic values of the potential curves $E_j(r)$, radial matrix elements $H_{jj'}(r)$ and $Q_{jj'}(r)$ at small r characterized by $l = 2j - 2 + |m|$ for even states ($\sigma = +1$) and $l = 2j - 1 + |m|$ for odd states ($\sigma = -1$) are given by expansion in powers of r with finite l, l':

$$E_j(r) = \bar{E}_j^{(0)} + \bar{E}_j^{(2)} r^2 + \sum_{k=1}^{[k_{\max}/4]} r^{4k} \bar{E}_j^{(4k)}, \qquad H_{jj'}(r) = \sum_{k=2}^{[k_{\max}/4]} r^{4k-2} \bar{H}_{jj'}^{(4k-2)},$$
$$Q_{jj'}(r) = \sum_{k=1}^{[k_{\max}/4]} r^{4k-1} \bar{Q}_{jj'}^{(4k-1)}, \qquad r \ll \min(l, l')\gamma/2. \tag{63}$$

Note that all

$$\bar{Q}_{jj'}^{(4k-1)} \equiv 0 \qquad \text{and} \qquad \bar{H}_{jj'}^{(4k-2)} \equiv 0 \quad \text{if} \quad |j - j'| > 2k. \tag{64}$$

The calculation was performed using the algorithm implemented in MAPLE up to $k_{\max} = 36$. Below we display several first coefficients of the matrix elements expansions:

$$\bar{E}_j^{(0)} = l(l+1), \qquad \bar{E}_j^{(2)} = \gamma m, \qquad \bar{E}_j^{(4)} = \frac{\gamma^2}{2} \frac{l^2 + l - 1 + m^2}{(2l-1)(2l+3)},$$
$$\bar{Q}_{jj+2}^{(3)} = \frac{\gamma^2}{2} \frac{\sqrt{(l+1)^2 - m^2}\sqrt{(l+2)^2 - m^2}}{\sqrt{2l+1}(2l+3)^2\sqrt{2l+5}},$$
$$\begin{aligned}\bar{H}_{jj}^{(6)} = \frac{\gamma^4}{2}&((16l^4 + 32l^3 + 248l^2 + 232l + 201)m^4 \\ &+ (-10l^2 - 224l^4 - 96l^5 + 118l - 288l^3 - 32l^6 - 195)m^2 + 16l^8 + 64l^7 \\ &+ 46l + 40l^6 - 127l^4 - 104l^5 + 71l^2 - 6l^3 - 6)/((2l-3)(2l-1)^4(2l+3)^4(2l+5)),\end{aligned}$$
$$\bar{H}_{jj+4}^{(6)} = \frac{-\gamma^4\sqrt{(l+1)^2 - m^2}\sqrt{(l+2)^2 - m^2}\sqrt{(l+3)^2 - m^2}\sqrt{(l+4)^2 - m^2}}{4\sqrt{2l+1}(2l+3)^2(2l+5)(2l+7)^2\sqrt{2l+9}}.$$
(65)

Such asymptotic behavior of the effective potentials allows us to find regular and bound solutions at $r \to 0$ that satisfied the boundary conditions (59).

3.3. Expansion of the regular solutions in power series

The asymptotics of the regular solutions $\chi_j^{(i_o)}(r) \equiv \chi_{ji_o}(r)$, $j = 1, \ldots, j_{\max}$, $i_o = 1, \ldots, N_o \leqslant j_{\max}$ of equation (58) are sought as expansions in powers of r up to an finite order $k_{\max}$:

$$\chi_{ji_o}(r) = c_{i_o} \sum_{k=0}^{k_{\max}} \chi_{ji_o}^{(k)} r^{\mu_{i_o}+k}, \qquad \chi_{ji_o}^{(0)} = \delta_{ji_o}, \qquad \chi_{ji_o}^{(k<0)} \equiv 0, \tag{66}$$

where c_{i_o} are normalized constants, μ_{i_o} is an unknown characteristic parameter. Substituting expansion (66) into (58) with equations (63)–(65) taken into account, we obtain the following

system of recurrence relations for the set of the unknown coefficients $\chi_{ji_o}^{(k)}$:

$$
\begin{aligned}
&-(l'+1+\mu_{i_o}+k)(\mu_{i_o}-l'+k)\chi_{ji_o}^{(k)} = 2Z\chi_{ji_o}^{(k-1)} - (m\gamma-\epsilon)\chi_{ji_o}^{(k-2)} \\
&-\sum_{s=4}^{k}\bar{E}_j^{(s)}\chi_{ji_o}^{(k-s)} - \sum_{s=4}^{k-2}\bar{H}_{jj}^{(s)}\chi_{ji_o}^{(k-s-2)} \\
&-\sum_{s=3}^{k-1}\sum_{j'=\max(1,i_o-[s/4]),j'\neq j}^{\min(j_{\max},i_o+[s/4])}(2l+2k-s)\bar{Q}_{jj'}^{(s)}\chi_{j'i_o}^{(k-s-1)} \\
&-\sum_{s=4}^{k-2}\sum_{j'=\max(1,i_o-[s/4]),j'\neq j}^{\min(j_{\max},i_o+[s/4])}\bar{H}_{jj'}^{(s)}\chi_{j'i_o}^{(k-s-2)},
\end{aligned}
\tag{67}
$$

where the indices l' and l are defined by

$$
l' = 2(j-1)+|m|+(1-\sigma)/2, \qquad l = 2(i_o-1)+|m|+(1-\sigma)/2. \tag{68}
$$

As follows from equations (66) and (67) at $k=0$, the conventional characteristic equation gives two roots for the unknown μ_{i_o}: $\mu_{i_o} = -l-1$ and $\mu_{i_o} = l$. The value $\mu_{i_o} = -l-1$ corresponds to irregular unbound solutions and is not considered here. The value $\mu_{i_o} = l$ corresponds to the required regular and bound solutions.

Note that the components of the vector $\left\{\chi_{ji_o}^{(k)}\right\}_{j=1}^{j_{\max}}$ at fixed i_o in the lhs of equation (67) is equal to zero if $j-i_o = k$. In this case we can put $\chi_{i_o+ki_o}^{(k)} = 0$, because this term will be determined as the leading term of the asymptotic form of the (i_o+k) th solution. A more detailed analysis of (67) with the account of (64) shows that the rhs of equation (67) is equal to zero and all $\chi_{ji_o}^{(k)}$ are equal to zero if $|j-i_o| > k/2$.

Thus, the system (67) can be solved sequentially for $k = 1, 2, \ldots, k_{\max}$. Below we display several first non-zero coefficients of the regular solutions expansions:

$$
\begin{aligned}
&\chi_{i_oi_o}^{(0)} = 1, \qquad \chi_{i_oi_o}^{(1)} = -\frac{Z}{l+1}, \qquad \chi_{i_oi_o}^{(2)} = -\frac{-2Z^2+(\epsilon-m\gamma)(l+1)}{2(l+1)(2l+3)}, \\
&\chi_{i_oi_o}^{(3)} = \frac{Z(-2Z^2+(\epsilon-m\gamma)(3l+4))}{6(l+1)(l+2)(2l+3)}, \\
&\chi_{i_o-2i_o}^{(4)} = \frac{\bar{Q}_{i_o-2i_o}^{(3)}(2l+5)}{6(2l+3)}, \\
&\chi_{i_oi_o}^{(4)} = \frac{\bar{E}_{i_o}^{(4)}}{4(2l+5)} + \frac{(\epsilon-m\gamma)^2}{8(2l+3)(2l+5)} + \frac{Z^4-Z^2(\epsilon-m\gamma)(3l+5)}{6(l+1)(l+2)(2l+3)(2l+5)}, \\
&\chi_{i_o+2i_o}^{(4)} = \frac{\bar{Q}_{i_o+2i_o}^{(3)}(2l+5)}{2(2l+7)}.
\end{aligned}
\tag{69}
$$

In the case of $\gamma = 0$ these coefficients transform into conventional ones for the expansion of the free regular Coulomb function $F_l(r)$ up to the factor r^{-1} with a known value of the coefficient $c_{i_o}(\gamma=0) = c_l$ from [20]. The latter gives us the opportunity to estimate the ratio $\left|c_{i_o}(\gamma)/c_{i_o}(0)\right|^2$ of a probability density, $\left|c_{i_o}(\gamma)\right|^2$, extracted from the calculated solution of equations (58)–(60) with boundary conditions (61) (or (62)) using asymptotic (66) and a free probability density, $\left|c_{i_o}(0)\right|^2$, in the vicinity of $r=0$.

3.4. Asymptotic form of basis functions and matrix elements at large r

Let us describe briefly the evaluation of the matrix elements at large r as expansions in powers of p^{-1} till the order of $k_{\max}$. For this purpose we use the eigenfunctions labeled by $\hat{v} = \overleftarrow{\rightarrow}$ and localized at large r in the vicinity of $\eta = \pm 1$ (see figure 3)

$$\Phi^{m\sigma=\pm 1}(\eta; r) = \frac{\Phi^{m\rightarrow}(\eta; r) \pm \Phi^{m\leftarrow}(\eta; r)}{\sqrt{2}}. \tag{70}$$

These functions have $N_\rho \equiv n = 0, 1, 2, \ldots$, nodes in the subintervals $0 < \eta < 1$ and $-1 < \eta < 0$, $N_\rho = N_\eta/2$ for even states, $\sigma = +1$ and $N_\rho = (N_\eta - 1)/2$ for the odd states, $\sigma = -1$, N_η being the number of nodes of $\Phi^{m\sigma}(\eta; r)$ in the interval $-1 < \eta < 1$ and the parity $\sigma = (-1)^{N_\eta}$. Note that $\Phi^{m\leftarrow}(\eta; r) = \Phi^{m\rightarrow}(-\eta; r)$ and $\Phi^{m\leftarrow}(\eta < 0; r) = \Phi^{m\rightarrow}(\eta > 0; r) = O(\exp(-p(1 + |\eta|))$ at $r \to \infty$ and $|\eta| \sim 1$ which will be used in the construction of the scattering wavefunctions defined by equation (105).

We find the matrix elements expanded in inverse powers of r with finite $j = n_l - 1$, $j' = n_r - 1$ and with the exponential terms omitted [22]

$$\begin{aligned} r^{-2}E_j(r) &= E_j^{(0)} + \sum_{k=1}^{k_{\max}} r^{-2k} E_j^{(2k)}, \qquad H_{jj'}(r) = \sum_{k=1}^{k_{\max}} r^{-2k} H_{jj'}^{(2k)}, \\ Q_{jj'}(r) &= \sum_{k=1}^{k_{\max}} r^{-2k+1} Q_{jj'}^{(2k-1)}, \qquad r \gg \max(n_l, n_r)\gamma/2. \end{aligned} \tag{71}$$

The calculation was performed using the algorithm describing in appendix A and implemented in MAPLE up to $k_{\max} = 8$. Below we display the first several coefficients of the potential curves $E_j(r)$ at fixed m:

$$\begin{aligned} E_j^{(0)} &= \gamma(2n + |m| + m + 1), \\ E_j^{(2)} &= -2n^2 - 2n - 1 - 2|m|n - |m|, \\ E_j^{(4)} &= (2\gamma)^{-1}(-4n^3 - 6n^2 - 4n - 6|m|n^2 - 6|m|n - 2m^2 n - 2|m| - m^2 - 1), \end{aligned} \tag{72}$$

and the matrix elements $Q_{jj'}(r)$, $H_{jj'}(r)$:

$$\begin{aligned} Q_{jj'}^{(1)} &= (n_r - n_l)\sqrt{n + 1}\sqrt{n + |m| + 1}\,\delta_{|n_l - n_r|,1}, \\ Q_{jj'}^{(3)} &= (4\gamma)^{-1}(n_r - n_l)\sqrt{n + 1}\sqrt{n + |m| + 1}\big(2(2n + |m| + 2)\delta_{|n_l - n_r|,1} \\ &\quad + \sqrt{n + 2}\sqrt{n + |m| + 2}\,\delta_{|n_l - n_r|,2}\big), \\ H_{jj'}^{(2)} &= (2n^2 + 2n + 2|m|n + |m| + 1)\delta_{|n_l - n_r|,0} \\ &\quad - \sqrt{n + 1}\sqrt{n + |m| + 1}\sqrt{n + 2}\sqrt{n + |m| + 2}\,\delta_{|n_l - n_r|,2}, \end{aligned} \tag{73}$$

$$\begin{aligned} H_{jj'}^{(4)} &= \gamma^{-1}\big((2n + |m| + 1)(2n^2 + 2n + 2|m|n + |m| + 2)\delta_{|n_l - n_r|,0} \\ &\quad + \sqrt{n + 1}\sqrt{n + |m| + 1}(n^2 + 2n + |m|n + |m| + 2)\delta_{|n_l - n_r|,1} \\ &\quad - \sqrt{n + 1}\sqrt{n + |m| + 1}\sqrt{n + 2}\sqrt{n + |m| + 2}(2n + |m| + 3)\delta_{|n_l - n_r|,2} \\ &\quad - \sqrt{n + 1}\sqrt{n + |m| + 1}\sqrt{n + 2}\sqrt{n + |m| + 2}\sqrt{n + 3}\sqrt{n + |m| + 3}\,\delta_{|n_l - n_r|,3}\big), \end{aligned} \tag{74}$$

where $n = \min(n_l, n_r)$. Note that all $Q_{jj'}^{(2k+1)} \equiv 0$ and $H_{jj'}^{(2k)} \equiv 0$ if $|j - j'| > k + 1$. Moreover, for second-order coefficients the identity $E_j^{(2)} + H_{jj}^{(2)} = 0$ takes place, i.e., at large r the centrifugal terms are eliminated from equation (58). It means that the leading terms

of the radial solutions $\chi_{ji_o}(r)$ have the asymptotic form of the Coulomb functions with zero angular momentum. If the scaled radial variable $\hat{r}$ is used, we put $\gamma = 1$ and use the effective charge $\hat{Z}$ and the scaled energy $\hat{\epsilon} = \epsilon/\gamma$ or $\hat{E} = E/\gamma$ in the above expressions. Note that the convergence domain of expansions (63) and (71) at small and large r is limited to the range of avoided crossing of the eigenvalues and maxima of the matrix elements versus r (see figures 4–7), that correspond to the known branching points in the complex plane of the parameter p [30]. This remark can be taken into account in the construction of the corresponding asymptotic solutions. To show explicitly the region where expansion (71) is valid the asymptotic values of potentials and matrix elements are displayed by dotted lines in figures 4–7. One can compare them with the corresponding numerical values calculated as mentioned above by the computer relative accuracy in the finite interval of the radial variable. The exponentially small corrections improving the convergence can be calculated by means of the additional series expansion of the solution in the region $D_2 = [0, 1-\eta_2]$, $\eta_2 < \eta_1$, $\eta_2 = o(p^{-1/2-\varepsilon})$ [24].

3.5. Asymptotic radial solution with exponential and inverse power series

The radial solutions $\chi_j^{(i_o)}(r) \equiv \chi_{ji_o}(r)$, $j = 1, \ldots, j_{\max}$, $i_o = 1, \ldots, N_o \leqslant j_{\max}$ of equation (58) at large r without the centrifugal terms (i.e., with zero angular momentum) have the asymptotic form

$$\chi_{ji_o}^{(as)}(r) = \frac{\exp(\imath p_{i_o} r + \imath\zeta \ln(2p_{i_o} r) + \imath\delta_{i_o}^c)}{2r\sqrt{p_{i_o}}}\delta_{ji_o}, \tag{75}$$

where p_{i_o} is the relative momentum in the channel, $\zeta \equiv \zeta_{i_o}$ is a Zommerfeld-type parameter, $\delta_{i_o}^c = \arg\Gamma(1-\imath\zeta)$ is the phase defined by the known Coulomb phase shift. The values of these characteristic parameters will be adapted to find the formal asymptotic solutions expanding the functions $\phi_{ji_o}(r)$ in inverse powers of r:

$$\chi_{ji_o}(r) = \phi_{ji_o}(r)\chi_{i_oi_o}^{(as)}(r), \qquad \phi_{ji_o}(r) = \sum_{k=0}^{k_{\max}} \phi_{ji_o}^{(k)} r^{-k}. \tag{76}$$

Substituting expansion (76) into equation (58) and equating the coefficients at the same powers of r we arrive at the recurrence relations for the unknown coefficients $\phi_{ji_o}^{(k)}$ [22]

$$\begin{aligned}
&\left(p_{i_o}^2 - 2E + E_j^{(0)}\right)\phi_{ji_o}^{(k)} + (2p_{i_o}\zeta - 2Z + 2\imath p_{i_o}(k-1))\phi_{ji_o}^{(k-1)} \\
&\qquad + (\zeta - 2\imath + \imath k)(\zeta - \imath + \imath k)\phi_{ji_o}^{(k-2)} + \sum_{k'=1}^{k}\left(E_j^{(k')} + H_{jj}^{(k')}\right)\phi_{ji_o}^{(k-k')} \\
&= \sum_{j'=1, j'\neq j}^{j_{\max}} \sum_{k'=1}^{k}\left(-2\imath p_{i_o} Q_{jj'}^{(k')} + (2k - k' - 1 - 2\imath\zeta)Q_{jj'}^{(k'-1)} - H_{jj'}^{(k')}\right)\phi_{j'i_o}^{(k-k')}.
\end{aligned} \tag{77}$$

From the first three equations of the set (77) for $\phi_{i_oi_o}^{(0)}$, $\phi_{j_0i_o}^{(0)}$, $\phi_{i_oi_o}^{(1)}$ we get the leading terms of the eigenfunction, the eigenvalue of the relative momentum, p_{i_o}, and the characteristic parameter, ζ, i.e., the initial data for solving the recurrence equations (77),

$$\phi_{j_0i_o}^{(0)} = \delta_{j_0i_o}, \qquad p_{i_o}^2 = 2E - E_{i_o}^{(0)} \to p_{i_o} = \sqrt{2E - E_{i_o}^{(0)}}, \qquad \zeta = \frac{Z}{p_{i_o}}. \tag{78}$$

For open channels $p_{i_o}^2 \geqslant 0$, while for closed channels $p_{i_o}^2 < 0$. Suppose there are $N_o \leqslant j_{\max}$ open channels, i.e., $p_{i_o}^2 \geqslant 0$ for $i_o = 1, \ldots, N_o$ and $p_{i_o}^2 < 0$ for $i_o = N_o + 1, \ldots, j_{\max}$. Substituting these initial data into the sequent equations of the set (77), we get a step-by-step

procedure for determining the coefficients $\phi_{ji_o}^{(k)}$ till $k = k_{\max}$. For example, for $k = 1$ the coefficients have the form

$$\phi_{j_1 i_o}^{(1)} = \frac{2\imath p_{i_o} Q_{j_1 i_o}^{(1)}}{E_{i_o}^{(0)} - E_{j_1}^{(0)}}, \qquad \phi_{i_o i_o}^{(1)} = \frac{\imath (Z^2 + \imath Z p_{i_o})}{2p_{i_o}^3} - \sum_{j_1 = \max(1, i_o - 1), j_1 \neq i_o}^{\min(j_{\max}, i_o + 1)} Q_{i_o j_1}^{(1)} \phi_{j_1 i_o}^{(1)}. \tag{79}$$

Substituting the asymptotic expressions (71) into equation (79), one can express the coefficients $\phi_{ji_o}^{(k)}$ explicitly via the number of the state (or of the channel) $i_o = n_o + 1$ and the number of the current equation $j = 1, \ldots, j_{\max}$. Note that if $j_{\max} \geqslant i_o + k$, then all nonzero terms in the sums in equations (79) will be included into the evaluation of each nonzero element $\phi_{ji_o}^{(k)}$ of the order k. The calculation was performed using the algorithm implemented in MAPLE up to $k_{\max} = 15$. For example, at $j_{\max} \geqslant i_o + k$ and $k = 0, 1$ the substitution of (73) into (79) yields

$$\begin{aligned}
&\phi_{i_o i_o}^{(0)} = 1, \\
&\phi_{i_o - 1 i_o}^{(1)} = \imath \frac{p_{i_o} \sqrt{n_o} \sqrt{n_o + |m|}}{\gamma}, \\
&\phi_{i_o i_o}^{(1)} = \left[\imath \frac{Z^2}{2p_{i_o}^3} - \frac{Z}{2p_{i_o}^2} \right] - \imath \frac{p_{i_o}(2n_o + |m| + 1)}{\gamma}, \\
&\phi_{i_o + 1 i_o}^{(1)} = \imath \frac{p_{i_o} \sqrt{n_o + 1} \sqrt{n_o + |m| + 1}}{\gamma}.
\end{aligned} \tag{80}$$

If we use the scaled radial variable $\hat{r}$, we put $\gamma = 1$ and use the effective charge $\hat{Z}$, the scaled energy $\hat{\epsilon} = \epsilon/\gamma$ and the momentum $\hat{p}_{i_o} = p_{i_o}/\sqrt{\gamma}$, $(\zeta = \hat{\zeta} = \hat{Z}/\hat{p}_{i_o})$ in the above expressions. For $\hat{r}_{\max} \gg \max\left(\hat{Z}^2/\left(2\hat{p}_{i_o}^2\right), n_o/2\right)$ we can use expansion (75) .

3.6. Asymptotic radial solution with Coulomb functions and inverse power series

Now let us consider the asymptotic solution $\chi_j^{(i_o)}(r) \equiv \chi_{ji_o}(r)$, $j = 1, \ldots, j_{\max}$, $i_o = 1, \ldots, N_o \leqslant j_{\max}$ of equation (58) following [32]:

$$\chi_{ji_o}(r) = R\left(p_{i_o}, r\right)\phi_{ji_o}(r) + \frac{\mathrm{d}R\left(p_{i_o}, r\right)}{\mathrm{d}r}\psi_{ji_o}(r), \tag{81}$$

where $R\left(p_{i_o}, r\right) = p_{i_o}^{-1/2} r^{-1}\left(\imath F_0\left(p_{i_o}, r\right) + G_0\left(p_{i_o}, r\right)\right)/2$, $F_0\left(p_{i_o}, r\right)$ and $G_0\left(p_{i_o}, r\right)$ are the Coulomb regular and irregular functions, respectively [20], that satisfy the condition

$$G_0\left(p_{i_o}, r\right)\frac{\mathrm{d}F_0\left(p_{i_o}, r\right)}{\mathrm{d}r} - \frac{\mathrm{d}G_0\left(p_{i_o}, r\right)}{\mathrm{d}r}F_0\left(p_{i_o}, r\right) = p_{i_o}. \tag{82}$$

The function $R\left(p_{i_o}, r\right)$ satisfies the differential equation

$$\frac{\mathrm{d}^2 R\left(p_{i_o}, r\right)}{\mathrm{d}r^2} + \frac{2}{r}\frac{\mathrm{d}R\left(p_{i_o}, r\right)}{\mathrm{d}r} + \left(p_{i_o}^2 + \frac{2Z}{r}\right) R\left(p_{i_o}, r\right) = 0. \tag{83}$$

Substituting function (81) into equation (58), using equation (83) and extracting the coefficients for the Coulomb function and its derivative, we arrive at an axillary set of two coupled differential equations with respect to the unknown functions $\phi_{ji_o}(r)\psi_{ji_o}(r)$ and the relative momentum p_{i_o} [22]. Then we expand the functions $\phi_{ji_o}(r)$ and $\psi_{ji_o}(r)$ in inverse powers of r:

$$\phi_{ji_o}(r) = \sum_{k=0}^{k_{\max}} \phi_{ji_o}^{(k)} r^{-k}, \qquad \psi_{ji_o}(r) = \sum_{k=0}^{k_{\max}} \psi_{ji_o}^{(k)} r^{-k}. \tag{84}$$

After substituting expansions (84) into these axillary equations and equating the coefficients at the same powers of r we arrive at the recurrence relations for the unknown coefficients $\phi_{ji_o}^{(k)}$ and $\psi_{ji_o}^{(k)}$:

$$\begin{aligned}
&\left(p_{i_o}^2 - 2E + E_j^{(0)}\right)\phi_{ji_o}^{(k)} - 2p_{i_o}^2(k-1)\psi_{ji_o}^{(k-1)} - (k-2)(k-3)\phi_{ji_o}^{(k-2)} \\
&\qquad - 2Z(2k-3)\psi_{ji_o}^{(k-2)} + \sum_{k'=1}^{k}\left(E_j^{(k')} + H_{jj}^{(k')}\right)\phi_{ji_o}^{(k-k')} \\
&\quad = \sum_{j'=1,\, j'\neq j}^{j_{\max}} \sum_{k'=1}^{k}\Big[\left((2k-k'-3)Q_{jj'}^{(k'-1)} - H_{jj'}^{(k')}\right)\phi_{j'i_o}^{(k-k')} \\
&\qquad + \left(2p_{i_o}^2 Q_{jj'}^{(k')} + 4ZQ_{jj'}^{(k'-1)}\right)\psi_{j'i_o}^{(k-k')}\Big],
\end{aligned} \tag{85}$$

$$\begin{aligned}
&\left(p_{i_o}^2 - 2E + E_j^{(0)}\right)\psi_{ji_o}^{(k)} + 2(k-1)\phi_{ji_o}^{(k-1)} - k(k-1)\psi_{ji_o}^{(k-2)} + \sum_{k'=1}^{k}\left(E_j^{(k')} + H_{jj}^{(k')}\right)\psi_{ji_o}^{(k-k')} \\
&\quad = \sum_{j'=1,\, j'\neq j}^{j_{\max}} \sum_{k'=1}^{k}\Big[\left((2k-k'+1)Q_{jj'}^{(k'-1)} - H_{jj'}^{(k')}\right)\psi_{j'i_o}^{(k-k')} - 2Q_{jj'}^{(k')}\phi_{j'i_o}^{(k-k')}\Big].
\end{aligned} \tag{86}$$

The summation indices $j_k, k = 0, 1, \ldots, k_{\max}$ possess integer values, except i_o and j_{k+1}, i.e., $j_k = 1, 2, \ldots, j_{\max}$, $j_k \neq i_o$, $j_k \neq j_{k+1}$. From the first four equations of the set (85) and (86) for $\phi_{i_oi_o}^{(0)}, \phi_{j_0i_o}^{(0)}, \psi_{i_oi_o}^{(0)}, \psi_{j_0i_o}^{(0)}$ we get the leading terms of the eigenfunction and eigenvalue of the relative momentum, p_{i_o}, i.e., the initial data for solving the recurrence equations (85) and (86),

$$\phi_{j_0i_o}^{(0)} = \delta_{j_0i_o}, \qquad \psi_{j_0i_o}^{(0)} = 0, \qquad p_{i_o}^2 = 2E - E_{i_o}^{(0)}, \tag{87}$$

that correspond to the leading term of $\chi_{ji_o}(r)$ satisfying the asymptotic expansion (75) at large r. Substituting these initial data into equations (85) and (86), we get a step-by-step procedure for the coefficients $\phi_{ji_o}^{(k)}$ and $\psi_{ji_o}^{(k)}$ till $k = k_{\max}$. For example, for $k = 1$ these coefficients have the form

$$\begin{aligned}
&\phi_{j_1i_o}^{(1)} = 0, \qquad \psi_{j_1i_o}^{(1)} = \frac{2Q_{j_1i_o}^{(1)}}{E_{i_o}^{(0)} - E_{j_1}^{(0)}}, \\
&\phi_{i_oi_o}^{(1)} = 0, \qquad \psi_{i_oi_o}^{(1)} = -\sum_{j_0=\max(1,i_o-1),\, j_0\neq i_o}^{\min(j_{\max},i_o+1)} Q_{i_oj_0}^{(1)}\psi_{j_0i_o}^{(1)}.
\end{aligned} \tag{88}$$

Substituting the asymptotic expressions (71) into equation (88), we get the explicit expression of the coefficients $\phi_{ji_o}^{(k)}$ and $\psi_{ji_o}^{(k)}$ via the number of the state (or of the channel) $i_o = n_o + 1$ and the number of the current equation $j = 1, \ldots, j_{\max}$. The calculation was performed using the algorithm implemented in MAPLE up to $k_{\max} = 15$. For example, at $j_{\max} \geqslant i_o + k$ and $k = 0, 1$, substituting (73) into (88) such elements take the form

$$\begin{aligned}
&\phi_{i_oi_o}^{(0)} = 1, \qquad \psi_{i_oi_o}^{(0)} = 0, \\
&\phi_{i_o-1i_o}^{(1)} = 0, \qquad \psi_{i_o-1i_o}^{(1)} = \frac{\sqrt{n_o}\,\sqrt{n_o + |m|}}{\gamma}, \\
&\phi_{i_oi_o}^{(1)} = 0, \qquad \psi_{i_oi_o}^{(1)} = -\frac{2n_o + |m| + 1}{\gamma}, \\
&\phi_{i_o+1i_o}^{(1)} = 0, \qquad \psi_{i_o+1i_o}^{(1)} = \frac{\sqrt{n_o + 1}\sqrt{n_o + |m| + 1}}{\gamma}.
\end{aligned} \tag{89}$$

If we use the scaled radial variable $\hat{r}$, we put $\gamma = 1$ and use the effective charge $\hat{Z}$ and the scaled momentum $\hat{p}_{i_o}$ $\left(\zeta = \hat{Z}/\hat{p}_{i_o}\right)$ in the above expressions.

Similar to [32], in each order k the recurrence relation (85) includes implicitly only the factor Z/p_{i_o}, while the recurrence relation (77) includes explicitly the quadratic factor $\left(Z/p_{i_o}\right)^2$. This allows us to expect that for small values of $\hat{p}_{i_o}$ or large values of the effective charge $\hat{Z}$ and, therefore, of the parameter $|\zeta| = |\hat{Z}/\hat{p}_{i_o}| \gg 1$, one can use expansion (81) at as substantially smaller distance $\hat{r}_{\max}/|\zeta|$ rather than expansion (75) at the essentially larger distance $\hat{r}_{\max}$.

Taking the convergence domain of the matrix elements into account, we find that the convergence domain of expansion (81) is $\hat{r}_{\max} \gg n_o/2$ and $\hat{r}_{\max} \gg \hat{Z}/\hat{p}_{i_o}(2n_o + |m| + 1)$, as follows from the asymptotic behavior of the matrix elements which does not depend on p_{i_o}. This is the main goal of expansion (81).

In addition, it should be noted that at large r the linearly independent matrix functions $\chi(r) \equiv \{\chi^{(i_o)}(r)\}_{i_o=1}^{N_o}$ of (76) and (81) satisfy the Wronskian-type relation

$$\mathbf{Wr}(\mathbf{Q}(r); \chi^*(r), \chi(r)) = \frac{\iota}{2}\mathbf{I}_{oo}, \tag{90}$$

where $\mathbf{Wr}(\bullet; \chi^*(r), \chi(r))$ is a generalized Wronskian with the long derivative defined as

$$\mathbf{Wr}(\bullet; \chi^*(r), \chi(r)) = r^2\left[(\chi^*(r))^T\left(\frac{\mathrm{d}\chi(r)}{dr} - \bullet\chi(r)\right) - \left(\frac{\mathrm{d}\chi^*(r)}{dr} - \bullet\chi^*(r)\right)^T\chi(r)\right]. \tag{91}$$

These relations are used to analyze the desirable accuracy of the above expansion [23].

3.7. Correspondence of asymptotic total wavefunctions at large r and |z|

To clarify the geometric sense of expansion (81) and (84) we recalculate the first four coefficients (88) and (89) for $j_{\max} \geqslant i_o + 1$ using the functions $|j\rangle = \tilde{\Phi}_j(\rho) = \lim_{r\to\infty,|\eta|\sim 1} r^{-1}\Phi_j(|\eta|; r)$ from (56):

$$\begin{aligned}
&\phi^{(1)}_{j_1 i_o} = 0,\\
&\psi^{(1)}_{j_1 i_o} = -\frac{1}{2}\langle j_1|\rho^2|i_o\rangle = \frac{\sqrt{n_o}\sqrt{n_o + |m|}}{\gamma}\delta_{j_1,i_o-1} + \frac{\sqrt{n_o + 1}\sqrt{n_o + |m| + 1}}{\gamma}\delta_{j_1,i_o+1},\\
&\phi^{(1)}_{i_o i_o} = 0, \qquad \psi^{(1)}_{i_o i_o} = -\frac{1}{2}\langle i_o|\rho^2|i_o\rangle = -\frac{2n_o + |m| + 1}{\gamma}.
\end{aligned} \tag{92}$$

Taking into account the orthogonality $\langle j|i_o\rangle = \left\langle\tilde{\Phi}^m_j(\rho)\middle|\tilde{\Phi}^m_{i_o}(\rho)\right\rangle = \delta_{ji_o}$ and completeness $\sum_j \left|\tilde{\Phi}^m_j(\rho')\right\rangle\left\langle\tilde{\Phi}^m_j(\rho)\right| = \delta(\rho' - \rho)$ of the basis functions (56), the asymptotic form of the total wavefunction at $p_{i_o}\rho^2/(2r) \ll 1$ can be written as

$$\begin{aligned}
\Psi^{m\hat{v}}(r, \eta) &= r\sum_j \left|\tilde{\Phi}^m_j(\rho)\right\rangle\left[\left\langle\tilde{\Phi}^m_j(\rho)\middle|\tilde{\Phi}^m_{i_o}(\rho)\right\rangle - \frac{1}{2r}\left\langle\tilde{\Phi}^m_j(\rho)\middle|\rho^2\middle|\tilde{\Phi}^m_{i_o}(\rho)\right\rangle\frac{\mathrm{d}}{\mathrm{d}r}\right]\chi^{(as)}_{i_o i_o}\left(p_{i_o}, r\right)\\
&= r\sum_j \left|\tilde{\Phi}^m_j(\rho)\right\rangle\left\langle\tilde{\Phi}^m_j(\rho)\right|\left[\left|\tilde{\Phi}^m_{i_o}(\rho)\right\rangle - \frac{1}{2r}\rho^2\left|\tilde{\Phi}^m_{i_o}(\rho)\right\rangle\frac{\mathrm{d}}{\mathrm{d}r}\right]\chi^{(as)}_{i_o i_o}\left(p_{i_o}, r\right)\\
&\approx r\tilde{\Phi}^m_{i_o}(\rho)\chi^{(as)}_{i_o i_o}\left(p_{i_o}, r(1 - \rho^2/(2r^2))\right) \approx \frac{1}{2}\tilde{\Phi}^m_{i_o}(\rho)X^{(+)}_{i_o i_o}(|z|)\exp\left(\iota\delta^c_{i_o}\right).
\end{aligned} \tag{93}$$

In the last transformation we use the relation $|z| = r(1-\rho^2/(2r^2)) + O(r^{-2})$ and the definitions (21), (57) and (27). Thus, the matrix of coefficients (81), (84) and (89) corresponds to the

overlap matrix between the asymptotic fundamental solutions (16) and (27) of equation (2) in cylindrical coordinates $z = r\cos\theta, \rho = r\sin\theta$ at large $|z|$ and the asymptotic basis functions of the independent variable $\eta = \cos\theta$ at large r. In appendix B we present detailed explanation of the effective approximation in the KM including the explicit construction of the corresponding effective mass and potentials versus the radial variable r and the results of calculation of their asymptotic values up to the order of r^{-4}.

4. Scattering states and photoionization cross sections

Consider the ejected electron above the first threshold $\epsilon_{m1}^{\rm th}(\gamma) = \epsilon_{m}^{\rm th}(\gamma) = \gamma(|m| + m + 1)$. We express the corresponding eigenfunction $\Psi_i^{Em\sigma}(r,\eta)$ of the continuous spectrum with the energy $\epsilon = 2E$ as

$$\Psi_i^{Em\sigma}(r,\eta) = \sum_{j=1}^{j_{\max}} \Phi_j^{m\sigma}(\eta;r)\hat{\chi}_{ji}^{(m\sigma)}(E,r), \qquad i = 1,\ldots,N_o, \tag{94}$$

where $\hat{\chi}^{(m\sigma)}(E,r)$ is the radial part of the 'incoming' or eigenchannel wavefunction. The normalization condition for $\Psi_i^{Em\sigma}(r,\eta)$ is

$$\begin{aligned}\left\langle \Psi_i^{Em\sigma}(r,\eta)\middle|\Psi_{i'}^{E'm'\sigma'}(r,\eta)\right\rangle &= \sum_{j=1}^{j_{\max}}\int_0^\infty r^2 dr\left(\hat{\chi}_{ji}^{(m\sigma)}(E,r)\right)^* \hat{\chi}_{ji'}^{(m'\sigma')}(E',r)\\ &= \delta(E-E')\delta_{mm'}\delta_{\sigma\sigma'}\delta_{ii'}.\end{aligned} \tag{95}$$

The function $\hat{\chi}^{(m\sigma)}(E,r)$ is expressed as

$$\hat{\chi}^{(m\sigma)}(E,r) = \sqrt{\frac{2}{\pi}}\chi^{(p)}(r)\mathbf{C}\cos\boldsymbol{\delta}. \tag{96}$$

The function $\chi^{(p)}(r)$ is a numerical solution of equation (58) that satisfies the 'standing-wave' boundary conditions (62) and has the standard asymptotic form [33]

$$\chi^{(p)}(r) = \chi^s(r) + \chi^c(r)\mathbf{K}, \qquad \mathbf{KC} = \mathbf{C}\tan\boldsymbol{\delta}, \qquad \mathbf{CC}^T = \mathbf{C}^T\mathbf{C} = \mathbf{I}_{oo}. \tag{97}$$

Here $\chi^s(r) = 2\,\mathrm{Im}(\chi(r))$ and $\chi^c(r) = 2\,\mathrm{Re}(\chi(r))$, $\chi(r)$ is the asymptotic solution defined in section 3.5 or 3.6, $\mathbf{K} \equiv \mathbf{K}_\sigma$ is the numerical short-range reaction matrix with the eigenvalue $\tan\boldsymbol{\delta}$ and the orthogonal matrix $\mathbf{C}$ of the corresponding eigenvectors. The regular and irregular functions satisfy the generalized Wronskian relation (91) at large r

$$\mathbf{Wr}(\mathbf{Q}(r);\chi^c(r),\chi^s(r)) = \mathbf{I}_{oo}. \tag{98}$$

Using $\mathbf{R}$-matrix calculus [21], we obtain the equation expressing the reaction matrix $\mathbf{K}$ via the matrix $\mathbf{R}$ at $r = r_{\max}$

$$\left(\mathbf{R}\chi^c(r) - \frac{\mathrm{d}\chi^c(r)}{\mathrm{d}r}\right)\mathbf{K} = \left(\frac{\mathrm{d}\chi^s(r)}{\mathrm{d}r} - \mathbf{R}\chi^s(r)\right). \tag{99}$$

When some channels are closed, the matrices in equation (99) are rectangular. Hence, the reaction matrix $\mathbf{K}$ may be presented as

$$\mathbf{K} = -\mathbf{X}^{-1}(r_{\max})\mathbf{Y}(r_{\max}), \tag{100}$$

where

$$\mathbf{X}(r) = \left(\frac{\mathrm{d}\chi^c(r)}{\mathrm{d}r} - \mathbf{R}\chi^c(r)\right)_{oo}, \qquad \mathbf{Y}(r) = \left(\frac{\mathrm{d}\chi^s(r)}{\mathrm{d}r} - \mathbf{R}\chi^s(r)\right)_{oo}, \tag{101}$$

are square $N_o \times N_o$ matrices.

The radial part of the 'incoming' wavefunction is expressed via the numerical 'standing' wavefunction and the short-range reaction matrix $\mathbf{K}$ by the relation

$$\hat{\chi}^{(m\sigma)}(E,r) = \sqrt{\frac{2}{\pi}}\chi^{-}(r) = \imath\sqrt{\frac{2}{\pi}}\chi^{(p)}(r)(\mathbf{I}_{oo} + \imath\mathbf{K})^{-1}, \tag{102}$$

and has the asymptotic form

$$\hat{\chi}^{(m\sigma)}(E,r) = \sqrt{\frac{2}{\pi}}(\chi(r) - \chi^{*}(r)\mathbf{S}^{\dagger}). \tag{103}$$

Here $\mathbf{S}$ is the short-range scattering matrix, expressed via the scattering matrix $\check{\mathbf{S}}_{\sigma}$ (31) and Coulomb phase shift δ^{c} as $\mathbf{S} \equiv \mathbf{S}_{\sigma} = \exp(-\imath\delta^{c})\check{\mathbf{S}}_{\sigma}\exp(-\imath\delta^{c})$, for which

$$\mathbf{S}^{\dagger}\mathbf{S} = \mathbf{S}\mathbf{S}^{\dagger} = \mathbf{I}_{oo}, \quad \mathbf{K} = \imath(\mathbf{I}_{oo} + \mathbf{S})^{-1}(\mathbf{I}_{oo} - \mathbf{S}), \quad \mathbf{S} = (\mathbf{I}_{oo} + \imath\mathbf{K})(\mathbf{I}_{oo} - \imath\mathbf{K})^{-1}. \tag{104}$$

The total wavefunction has the asymptotic form reverse to the common scattering problem, namely, 'incident wave + ingoing wave',

$$\Psi^{(-)}_{Em\hat{v}}(r,\eta) \equiv \Psi^{(-)}_{Em\overleftarrow{\rightarrow}}(r,\eta) = \tfrac{1}{\sqrt{2}}(\Psi^{Em\sigma=+1}(r,\eta) \pm \Psi^{Em\sigma=-1}(r,\eta))\exp(-\imath\delta^{c}), \tag{105}$$

that corresponds to the function (36) (see details in appendix C). Now the expression (38) for the cross section $\sigma^{d}_{Nlm}(\omega)$ of photoionization by the light linearly polarized along the axis z can be written as

$$\sigma^{d}_{Nlm}(\omega) = 4\pi^{2}\alpha\omega\sum_{i=1}^{N_o}\left|D^{m\sigma\sigma'}_{i,N,l}(E)\right|^{2}a_0^{2}, \tag{106}$$

where $D^{m\sigma\sigma'}_{i,N,l}(E) \equiv D^{m\sigma\sigma'}_{i,i',\nu'}(E)$ are the matrix elements of the dipole moment

$$D^{m\sigma\sigma'}_{i,i',\nu'}(E) = \left\langle\Psi^{Em\sigma=\mp1}_{i}(r,\eta)\middle|r\eta\middle|\Psi^{m\sigma'=\pm1}_{i'\nu'}(r,\eta)\right\rangle = \sum_{j=1}^{j_{\max}}\int_{0}^{r_{\max}} r^{2}\,\mathrm{d}r\,\hat{\chi}^{(m\sigma=\mp1)}_{ji}(E,r)d^{(m\sigma\sigma')}_{ji'\nu'}(r), \tag{107}$$

and $d^{(m\sigma\sigma')}_{ji'\nu'}(r)$ are the matrix elements of the partial dipole moments

$$d^{(m\sigma\sigma')}_{ji'\nu'}(r) = \sum_{j'=1}^{j_{\max}}\left\langle\Phi^{m\sigma=\mp1}_{j}(\eta;r)\middle|r\eta\middle|\Phi^{m\sigma'=\pm1}_{j'}(\eta;r)\right\rangle_{\eta}\chi^{(m\sigma'=\pm1)}_{j'i'\nu'}(r). \tag{108}$$

In the above expressions $\omega = E - E_{Nlm}$ is the frequency of radiation, $E_{Nlm} \equiv E_{m\sigma'i'\nu'}$ is the energy of the initial bound state $|Nlm\rangle = \Psi^{m\sigma'}_{i'\nu'}(r,\eta)$ below half of the first true threshold shift $\epsilon^{\mathrm{th}}_{m1}(\gamma)/2$ from formula (56) at $i' = 1$. The continuous spectrum solution $\chi^{(p)}(r)$ having the asymptotic form of a 'standing' wave and the reaction matrix $\mathbf{K}$ required for calculating (96) or (103), as well as the discrete spectrum solution $\chi(r)$ and the eigenvalue $E_{m\sigma'i'=1\nu'}$, can be calculated using the program KANTBP [33]. Figure 10 shows an example of the wavefunctions of the continuous spectrum calculated using equations (94)–(96) in the basis of functions (51) shown in figure 3 for $\sigma = -1$, $Z = 1$, $m = 0$ and $\gamma = 1$ with the energy $E = 1.7$ au above the second threshold $1/2\epsilon^{\mathrm{th}}_{m2} = 1.5$. One can see that equations (96) and (103) yield the same result when used to calculate the absolute value in equation (106), as well as equation (105) performing the summation over $\hat{v}$ in accordance with equation (38). Hence, equation (96) is preferable for using real arithmetic. For the light circularly polarized in the plane xOy similar expression can be written using (42) with $(\vec{e}_{\pm}\vec{r}) = \frac{r}{\sqrt{2}}\sqrt{1-\eta^{2}}\exp(\pm\imath\varphi)$.

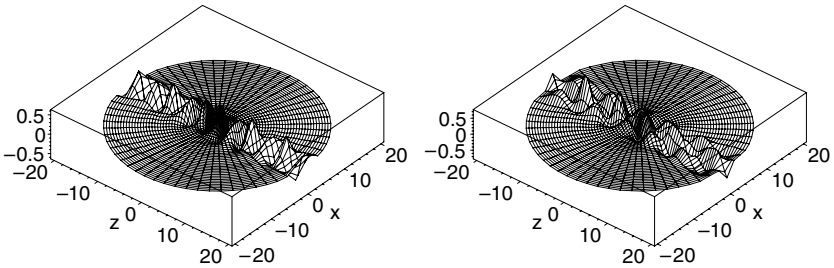

Figure 10. Profiles of wavefunctions Ψ_1 and Ψ_2 in the zx plane of the first (a) and the second (b) open channels having the asymptotic form (96) for $\sigma = -1, Z = 1, m = 0$ and $\gamma = 1$ with the energy $E = 1.7$ au above the second threshold $1/2\epsilon^{\rm th}_{m2} = 1.5$.

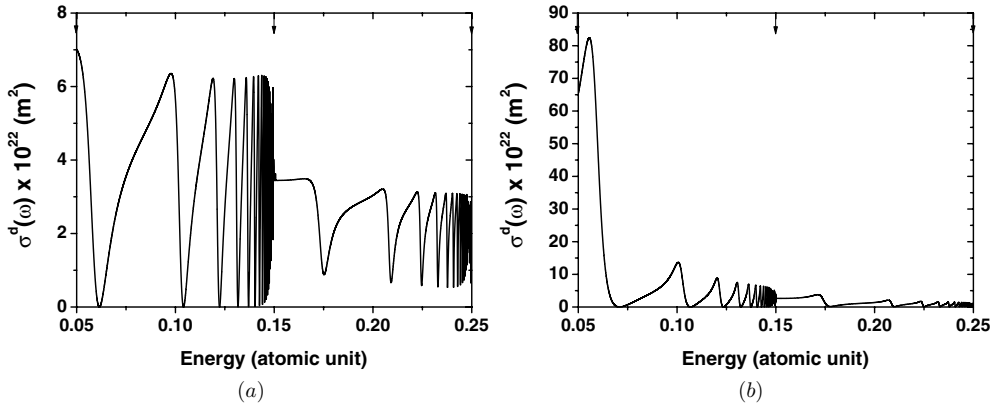

Figure 11. Cross sections of photoionization from the states $1s_0$ (a) and $3d_0$ (b) versus the energy for $\gamma = 1 \times 10^{-1}$, and for the final state with $\sigma = -1, Z = 1, m = 0$. The arrows indicate the successive Landau thresholds $E_j = 1/2\epsilon^{\rm th}_{mj}$ (71).

5. Numerical results and discussion

In our calculations we used the following values of the physical constants [34]: $1\ {\rm cm}^{-1} = 4.556\,33 \times 10^{-6}$ au, the Bohr radius $a_0 = 5.291\,77 \times 10^{-11}$ m and the fine-structure constant $\alpha = 7.297\,35 \times 10^{-3}$.

Figure 11 displays the calculated photoionization cross section from the states $1s_0$ and $3d_0$ at $B_0 = 2.35 \times 10^4 T$ ($\gamma = 1 \times 10^{-1}$) in the energy interval from $E = 0.05$ au to $E = 0.25$ au with the final state $\sigma = -1, m = 0$. We used ten eigenfunctions ($j_{\max} = 10$) of the problem (51)–(53) which requires to solve ten equations of the system (58). The finite element grids of $\hat{r} = \sqrt{\gamma} r$ have been chosen as 0 (200) 3 (200) 20 (200) 100 for the discrete spectrum and 0 (200) 3 (200) 20 (200) 100 (1000) 1000 for the continuous one. Enclosed in parentheses are the numbers of finite elements of the order $k = 4$ in each interval. The number of nodes in the grids is 2400 and 6401, so that the maximum number of unknowns in equation (58) is 24 000 and 64 010, respectively. Figure 12 displays the continuous spectrum states (in scaled coordinates) with the energies $E = 0.0596$ au and $E = 0.0903$ au that correspond to $\delta_o = 0$ and $\delta_o = \pi/2$, respectively. The corresponding series of quasi-stationary states imbedded in the continuum,

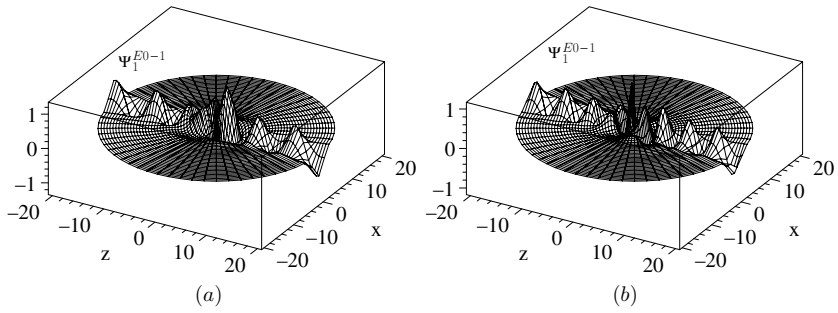

Figure 12. Profiles of the eigenfunctions $\Psi_1^{Em\sigma}$ in the zx plane of the continuous spectrum with $\sigma = -1$, $Z = 1$, $m = 0$ and $\gamma = 1 \times 10^{-1}$. The states with the energies $E = 0.0596$ au and $E = 0.0903$ au correspond to $\delta_o = 0$ and $\delta_o = \pi/2$, respectively.

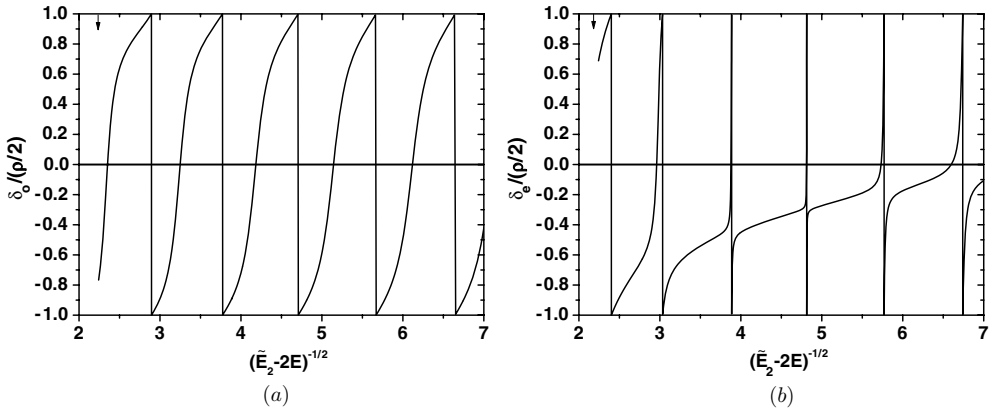

Figure 13. Phase shift δ of odd (a) and even (b) continuum states for $Z = 1$, $m = 0$ and $\gamma = 1 \times 10^{-1}$ versus $(\tilde{E}_2 - 2E)^{-1/2}$. The arrow points at the energy of the first Landau threshold $(\tilde{E}_2 - \tilde{E}_1)^{-1/2} = 5^{1/2} \approx 2.236$.

defined by the short-range phase shifts $\delta_o = n_o\pi + \pi/2$, are plotted in figure 13(a) versus $(\tilde{E}_2 - 2E)^{-1/2} = n_o + \Delta_{n_o}$, where $\tilde{E}_j = \epsilon_{mj}^{\text{th}}$. The existence of such states allows one to explain the nonmonotonic dependence of the photoionization cross section upon the energy between the thresholds. The short-range phase shifts $\delta_e = n_e\pi + \pi/2$ of the even continuum states are plotted in figure 13(b) versus $(\tilde{E}_2 - 2E)^{-1/2} = n_e + \Delta_{n_e}$. The corresponding transmission $|\hat{\mathbf{T}}|^2 = \sin^2(\delta_e - \delta_o)$ and reflection $|\hat{\mathbf{R}}|^2 = \cos^2(\delta_e - \delta_o)$ coefficients (31) versus the energy E (a) and $(\tilde{E}_2 - 2E)^{-1/2}$ (b) are shown in figure 14. Nonmonotonic behavior of $|\hat{\mathbf{T}}|$ and $|\hat{\mathbf{R}}|$ is seen to include the cases of resonance transmission $|\hat{\mathbf{T}}| = 1$ and $|\hat{\mathbf{R}}| = 0$ and total reflection $|\hat{\mathbf{T}}| = 0$ and $|\hat{\mathbf{R}}| = 1$. As an example, we display the absolute values of the total wavefunctions (105) of the continuous spectrum $\boldsymbol{\Psi}_{Em\rightarrow}^{(-)}$ and $\boldsymbol{\Psi}_{Em\leftarrow}^{(-)}$ in figure 15 (in scaled coordinates). The profiles of the states with the energy $E = 0.05885$ au and $E = 0.11692$ au demonstrate the resonance transmission and total reflection, respectively. They agree with appendix C and with the proper longitudinal solutions combined with the left and right basis functions (see figures 2(b) and 5).

Figure 16 demonstrates the dependence on the energy E (a) and $(\tilde{E}_2 - 2E)^{-1/2}$ (b) of the following quantities: the squared modulus of the matrix element (SMME) $\breve{T}_{11} = S_{11} - 1$,

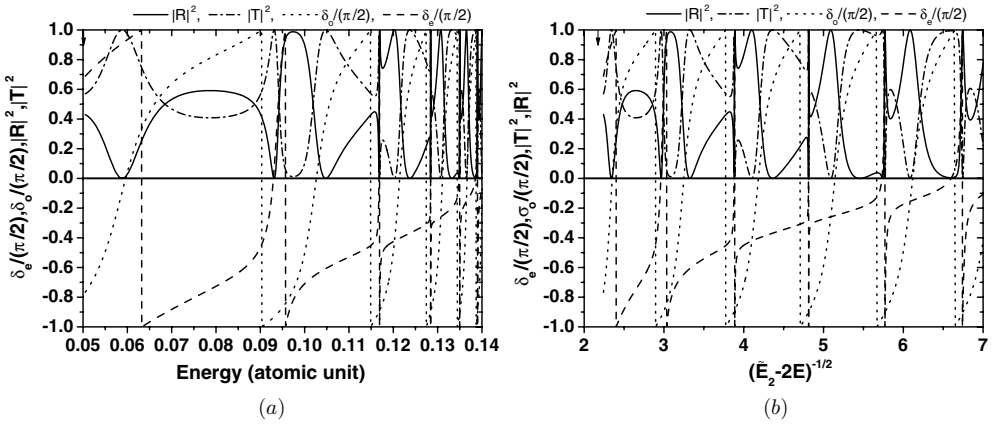

Figure 14. Transmission $|\hat{\mathbf{T}}|^2$ and reflection $|\hat{\mathbf{R}}|^2$ coefficients, even δ_e and odd δ_o phase shifts versus the energy E (a) and $(\tilde{E}_2 - 2E)^{-1/2}$ (b) for continuum states with $Z = 1, m = 0$ and $\gamma = 1 \times 10^{-1}$.

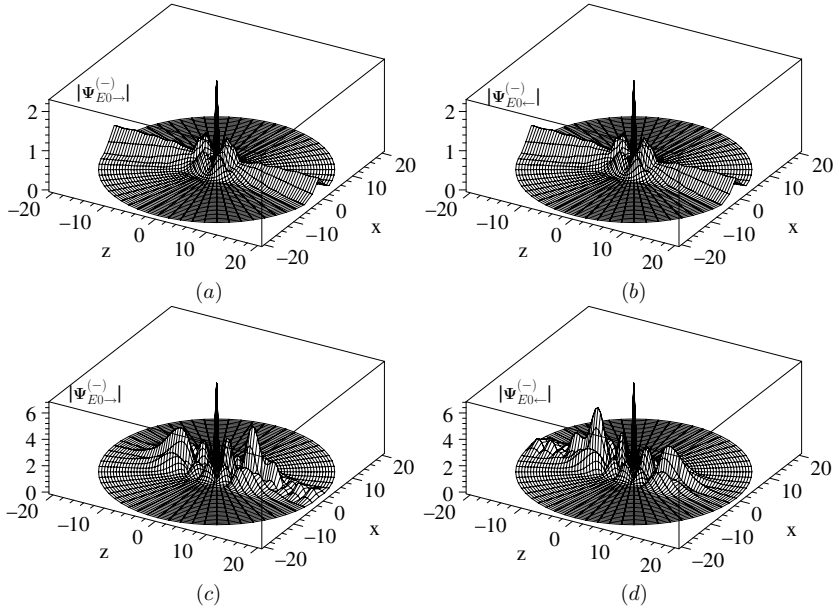

Figure 15. Profiles of total wavefunctions $|\Psi^{(-)}_{Em\rightarrow}|$ (a, c) and $|\Psi^{(-)}_{Em\leftarrow}|$ (b, d) in the zx plane of the continuous spectrum with $Z = 1, m = 0$ and $\gamma = 1 \times 10^{-1}$. The states with the energy $E = 0.05885$ au (a, b) correspond to the resonance transmission, while those with the energy $E = 0.11692$ au (c, d) correspond to the total reflection.

characterizing the elastic scattering of the electron, the odd phase shift (OPS) δ_o, and the cross section $\sigma^d(\omega)$ (106) of photoionization from the initial even state $1s_0$ $((Nlm) = (100))$ with the energy $E_{100} = -0.497\,526\,480\,40$ au, $\omega = E - E_{100}$ being the frequency of radiation. The final scattering state with $\sigma = -1$ and $m = 0$ in the magnetic field $B_0 = 2.35 \times 10^4$ T $(\gamma = 1 \times 10^{-1})$ is considered. The first two quantities are normalized to fit the plot

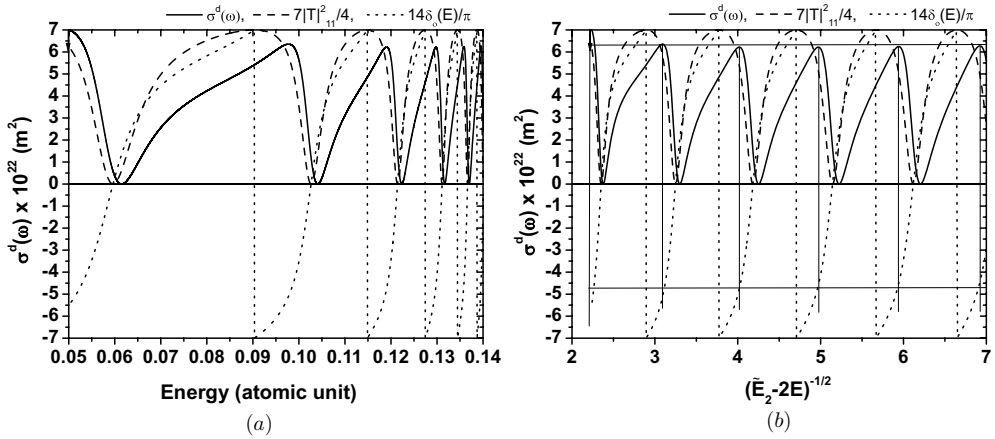

Figure 16. Squared modulus of the matrix element $\check{T}_{11}$, multiplied by $7/4$, odd phase shift δ_o multiplied by $14/\pi$ and cross section $\sigma^d(\omega)$ (106) of photoionization from the initial state $1s_0$ versus the energy E (a) and $(\tilde{E}_2 - 2E)^{-1/2}$ (b) for the final scattering state with $\sigma = -1$, $Z = 1$, $m = 0$ and $\gamma = 1 \times 10^{-1}$.

range. The comparison of the three curves shows that the maxima of the SMME of elastic scattering coincide with the jumps of the OPS. The minima of SMME coincide with zeros of OPS exactly, while the minima of the photoionization cross section (PCS) occur with some delay. Figure 16(b) shows that in the scale $(\tilde{E}_2 - 2E)^{-1/2}$ SMME is periodical, while PCS is quasi-periodical. The maxima of PCS occur after each phase jump when the OPS has approximately the same value of $-0.35/\pi$, while the maxima of SMME coincide exactly with these jumps that, as mentioned above, correspond to quasi-stationary states imbedded in the continuum. The minima of PCS correspond approximately to the same value $0.1/\pi$ of the phase. The figures show only the first fragment of the infinite sequence of maxima and minima that corresponds to the existence of the infinite and countable series of Coulomb quasi-stationary states below the second threshold, induced by the confinement potential of the magnetic field, in accordance with the multichannel quantum defect theory.

For the initial state $1s_0$ in the whole energy interval the results are in good agreement with those of **R**-matrix calculations within the frameworks of the multichannel quantum defect theory [6]. We also compared our results with those of the complex-rotation method using the expansion over the basic set of 10 000 complex spherical Sturmian-type functions [11] and the basic set of 450 mixed Slater-Landau functions [8]. In this case the agreement is good only between the thresholds, but not near them. The agreement with [6] proves that our method is valid to describe the true threshold behavior of the photoionization cross section, i.e., one of the goals of elaborating the new approach is achieved.

Figure 17 displays the cross section of photoionization by the light linearly polarized along the axis z from the vibrational state $3d_0$ (a) and the rotational state $3s_0$ (b) at $B_0 = 6.10$ T ($\gamma = 2.595 \times 10^{-5}$) in the energy interval between $E = 6.0\ \mathrm{cm}^{-1}$ and $E = 8.0\ \mathrm{cm}^{-1}$. In this case we increased $j_{\max}$ up to 35 and the finite element grids of $\hat{r} = \sqrt{\gamma} r$ were chosen as 0 (200) 0.03 (200) 0.2 (200) 1 for the discrete spectrum and 0 (200) 0.03 (200) 0.2 (200) 1 (2000) 100 (4000) 1000 for the continuous one. The number of nodes in these grids is 2400 and 26 401, respectively. The corresponding maximal number of unknowns in equation (58) is 84 000 and 924 035. Figure 18(a) shows the absolute maximum values of the continuum wavefunctions $\hat{\chi}^{(01)}_{j1}(E, \hat{r})$ at $E = 6.0\ \mathrm{cm}^{-1}$. We calculated the cross sections with the

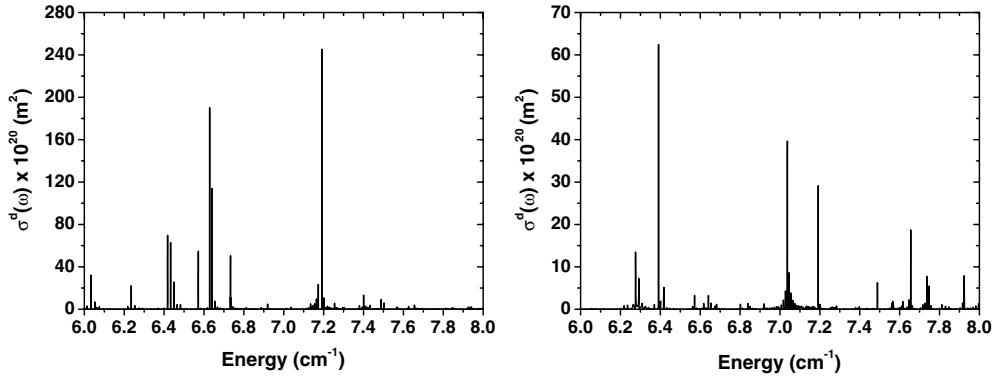

Figure 17. The cross section of photoionization from the states $3d_0$ (*a*) and $3s_0$ (*b*) versus the energy for $\gamma = 2.595 \times 10^{-5}$ and for the final state with $\sigma = -1$, $Z = 1$, $m = 0$.

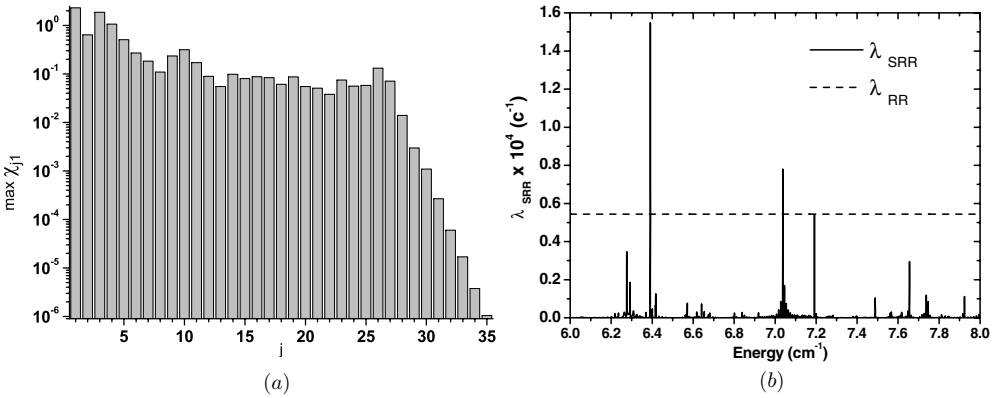

Figure 18. (*a*) Absolute maximum values, max χ_{j1}, of the continuum wavefunctions $\hat{\chi}^{(01)}_{j1}(E, \hat{r})$ at $\gamma = 2.595 \times 10^{-5}$, $E = 6.0\ \mathrm{cm}^{-1}$ and $j_{\max} = 35$. (*b*) Laser-stimulated radiative recombination rate into the bound state $N' = 3$, $l' = 0$, $m' = 0$ versus the energy of the initially free positron.

energy step $5 \times 10^{-4}\ \mathrm{cm}^{-1}$ in all the region except the vicinity of peaks, where the step was $5 \times 10^{-6}\ \mathrm{cm}^{-1}$.

The relation between the photoionization cross section and the induced radiative recombination rate [5] makes it possible to apply the results of this section to an urgent problem of the production of cold antihydrogen atoms in magnetic traps [3]. The idea is to use the resonances due to the quasi-stationary states arising in the magnetic field in order to enhance the laser-induced radiative recombination into a given bound state by choosing the proper laser frequency. Let us consider the recombination into the state $N' = 3, l' = 0, m' = 0$, that may be stimulated by a titanium-sapphire laser, under the conditions typical for positron–antiproton plasma in magnetic traps used for antihydrogen production, namely, the temperature of the plasma $T = 4$ K, the positron density $n_e = 1 \times 10^8\ \mathrm{cm}^{-3}$, the magnetic induction $B = 6.10$ T. The laser intensity is taken such that at 4 K without the magnetic field the rate of induced recombination is equal to that of the spontaneous one. In particular , for $N = 3$

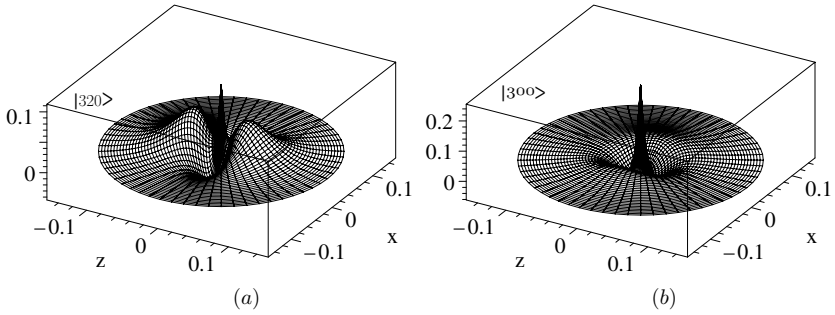

Figure 19. Profiles of the wavefunctions in the zx plane of the bound states $|Nlm\rangle$ with $\sigma = +1$, $Z = 1$ and $\gamma = 2.595 \times 10^{-5}$: ($a$) the vibrational state $|320\rangle$ with the minimal energy correction; (b) the rotational state $|300\rangle$ with the maximal energy correction.

this intensity is $I = 24$ W cm^{-2} [4]. Figure 18(b) shows the dependence of the laser-stimulated recombination rate per one antiproton λ_{SRR} upon the initial energy of the positron $E = E_{Nlm} + \omega$. For comparison the horizontal dashed line displays the rate λ_{RR} of the spontaneous radiative recombination into all the states with $N = 3$, which at the intensity considered is equal to the rate of the laser-stimulated recombination without the magnetic field. Obviously, there are narrow resonances for which the rate of recombination into the state with fixed $l = 0$, $m = 0$ in magnetic field is appreciably higher than the rate of recombination into all nine states with different l and m possible for $N = 3$ without the magnetic field.

Note that states $3d_0$, $3p_0$ and $3s_0$ with energies $E_{320} = -0.055\,555\,552\,07$ au, $E_{310} = -0.055\,555\,549\,49$ au and $E_{300} = -0.055\,555\,542\,37$ au, respectively, are nearly degenerate. To calculate these energies we used three equations of the system (58) ($j_{\max} = 3$); increasing $j_{\max}$ keeps them stable. We also compared the energies with those calculated by means of the second-order algebraic perturbation theory [35]. The results coincide with each other to the 13th digit. The wavefunctions of the bound states $|Nlm\rangle$ with even parity $\sigma = +1$ in a homogenous magnetic field are shown in figure 19. Values of functions scaled by factor $\gamma^{3/4}$ versus scaled coordinates $\hat{r}$. From here one can find an evident explanation of the fact that the cross section of photoionization by the light linearly polarized along the axis z (see figure 17) from the vibrational state $3d_0$ distributed along the z axis exceeds in four times the cross section from the rotational state $3s_0$ distributed along the x axis.

6. Conclusions

A new efficient method for calculating both the discrete and the continuous spectrum wavefunctions of a hydrogen atom in a strong magnetic field is developed based on the Kantorovich approach to the parametric eigenvalue problems in spherical coordinates. The 2D spectral problem for the Schrödinger equation with fixed magnetic quantum number and parity is reduced to a 1D spectral parametric problem for the angular variable and a finite set of ordinary second-order differential equations for the radial variable. The rate of convergence is analyzed numerically and is illustrated with a number of typical examples. The results are in good agreement with calculations of photoionization cross sections by other authors. It is shown that the calculated photoionization cross sections has the true threshold behavior and that the recombination cross sections can be recalculated using the relations presented. The recurrence relations for the calculation of the coefficients of asymptotic expansions of

fundamental solutions of a set of the radial equations or the overlap matrix open the way to study the threshold phenomena using the known asymptotic expansion of Coulomb functions [36, 37].

The main advantages of the elaborated approach from the calculation and the theoretical viewpoints consist of the following.

The calculations on all steps of the Kantorovich approach are realized with the help of stable calculation schemes and with prescribed accuracy. The economy of computer resources is achieved by means of analytic calculation of all needed asymptotic forms of adaptive basis functions, matrix elements of radial coupling and radial solutions, which makes it possible to reduce the interval of integration in the corresponding boundary problems.

For the first time resonance transmission and total reflection effects for scattering processes of electrons on protons in a homogenous magnetic field are manifested.

The approach developed provides a useful tool for calculations of threshold phenomena in the formation and ionization of (anti)hydrogen-like atoms and ions in magnetic traps, quantum dots in magnetic field [38], channeling processes [39] and potential scattering with confinement potentials [40].

Acknowledgments

The authors thank Professors A G Abrashkevich, A M Ermolaev, V S Melezhik and V V Pupyshev for an useful discussion. This work was partly supported by Grant I-1402/2004-2007 of the Bulgarian Foundation for Scientific Investigations, the theme 09-6-1060-2005/2009 'Mathematical support of experimental and theoretical studies conducted by JINR' and Scientific Center for Applied Research of JINR. A part of this work was carried out within the framework of the Russian Analytical Departmental Objective Program 'Development of the Scientific Potential of the Higher School' (2006–2008), project RNP.2.1.1.4473 'Mesooptics' and supported by the grant CRDF BRHE REC-006 SR-006-X1/B75M06 Y3-P-06-08.

Appendix A. Asymptotic expansions of basis functions and matrix elements at large *r*

Following [20, 24], at step 1 we change the coordinate $\eta \in [0, 1]$ (or $\eta \in [-1, 0]$) for the new coordinate y according to

$$y = 2p(1 - \eta) \quad (\text{or } y = 2p(1 + \eta)). \tag{A.1}$$

For our purposes it is sufficient to consider $\eta \in [0, 1]$. We suppose that the coordinate y lies in the interval corresponding to $\eta \in D_1$, $D_1 = [1 - \eta_1, 1]$, $\eta_1 = o(p^{1/2-\epsilon})$, $0 < \epsilon < 1/2$. Now the eigenvalue problem (54) takes the form

$$\left[(y^2 - 4py)\frac{\partial^2}{\partial y^2} + (2y - 4p)\frac{\partial}{\partial y} - \left(\frac{16p^2(m^2 + y^2) + y^3(y - 8p)}{4y(y - 4p)} + \lambda_n\right)\right]\Phi_j(y) = 0. \tag{A.2}$$

The corresponding matrix elements (60) read as

$$Q_{jj'}(r) = -I_{01;jj'}(r), \qquad H_{jj'}(r) = I_{11;jj'}(r). \tag{A.3}$$

where the integrals $I_{dd';jj'}(r)$ with $d, d' = 0, 1$ are calculated as follows:

$$I_{dd';jj'}(r) = \frac{1}{2p}\int_0^{2p} \mathrm{d}y \left[\left(\frac{\partial}{\partial r} + \frac{2y}{r}\frac{\partial}{\partial y}\right)^d \Phi_j(y)\right]\left[\left(\frac{\partial}{\partial r} + \frac{2y}{r}\frac{\partial}{\partial y}\right)^{d'} \Phi_{j'}(y)\right]. \tag{A.4}$$

In these expressions the asymptotic quantum number n denotes the transversal quantum numbers that are connected with the unified numbers j and j' as $n_l = j - 1$ and $n_r = j' - 1$. At steps 2–3 from the set of functions $\Phi_j(y)$ we turn to the set of functions $F_n(y)$

$$\Phi_j(y) = f_m(y)F_n(y), \qquad f_m(y) = \exp\left(-\frac{y}{2}\right) y^{|m|/2} \left(1 - \frac{y}{4p}\right)^{|m|/2}, \tag{A.5}$$

the latter presented as a sum of the associated Laguerre polynomials [20]

$$F_n(y) = (2p)^{1/2} \sum_s C_n(s, r) L^{|m|}_{n+s}(y). \tag{A.6}$$

Using the knowing properties of the associated Laguerre polynomials [20], we find that the coefficients $C_n(s, r)$ satisfy the recurrence relations

$$\begin{aligned}\left(n + s + \frac{|m| + 1}{2} - \frac{\lambda_n + 2(n + s)^2 + 2(n + s)(|m| + 1) + |m| + 1}{4p}\right) C_n(s, r) \\ + \frac{(n + s + 1)(s + 1 + n + |m|)}{4p} C_n(s + 1, r) \\ + \frac{(s + n)(s + |m| + n)}{4p} C_n(s - 1, r) = 0.\end{aligned} \tag{A.7}$$

As a result of this step we get the matrix elements as a sum of integrals with the associated Laguerre polynomials

$$I_{dd';jj'}(r) = \sum_{s_l s_r} \int_0^{2p} \mathrm{d}y f_m^2(y) \widetilde{C}^{(d)}_{n_l,s_l} \widetilde{C}^{(d')}_{n_r,s_r}, \tag{A.8}$$

where the coefficients $\widetilde{C}^{(d)}_{n_r,s_r}$ are obtained by differentiation of (A.5) and (A.6) and formation of a given weight factor, $f_m^2(y)$, such that

$$\begin{aligned}\widetilde{C}^{(0)}_{n_l,s_l} &= C_{n_l}(s_l, r) L^{|m|}_{n_l+s_l}(y), \qquad \widetilde{C}^{(0)}_{n_r,s_r} = C_{n_r}(s_r, r) L^{|m|}_{n_r+s_r}(y), \\ \widetilde{C}^{(1)}_{n_r,s_r} &= \frac{\mathrm{d}C_{n_r}(s_r, r)}{\mathrm{d}r} L^{|m|}_{n_r+s_r}(y) + \frac{C_{n_r}(s_r, r)}{r}\big[(n_r + s_r + 1) L^{|m|}_{n_r+s_r+1}(y) \\ &\quad - (n_r + s_r + |m|) L^{(m|}_{n_r+s_r-1}(y)\big].\end{aligned} \tag{A.9}$$

At step 4 for the evaluation of the integrals (A.8) we change the domain from $[0, 2p]$ to $[0, \infty)$ and then omit the exponentially small terms. Using the approximated relation up to the order of $k_{\max} < |m|$, that is exact if $k_{\max} \geqslant |m|$

$$\left(1 - \frac{y}{4p}\right)^{|m|} = \sum_{k=0}^{k_{\max}} \frac{|m|!}{k!(|m| - k)!} \left(\frac{y}{4p}\right)^k + O((4p)^{-k_{\max}-1}), \tag{A.10}$$

and the orthonormality condition for the associated Laguerre polynomials

$$\int_0^\infty \mathrm{d}y \exp(-y) y^{|m|} L^{|m|}_{n_l+s_l}(y) L^{|m|}_{n_r+s_r}(y) = \frac{(n_l + s_l + |m|)!}{(n_l + s_l)!} \delta_{n_l+s_l,n_r+s_r}, \tag{A.11}$$

we obtain the matrix elements in the algebraic form. For example, if $k_{\max} = 1$ the matrix element $I_{00;jj} \equiv I_{jj} \equiv 1$ takes the form

$$I_{00;jj}(r) = \sum_s \left[1 - \frac{|m|(2n + 2s + |m| + 1)}{4p}\right] C_n(s, r)^2 \frac{(n + s + |m|)!}{(n + s)!}. \tag{A.12}$$

At step 5 we expand $C_n(s,r)$ and λ_n as

$$C_n(s,r) = c_{s,n}^{(0)} + \sum_{k=1}^{k_{\max}} \left(\frac{1}{4p}\right)^k c_{s,n}^{(k)}, \qquad \lambda_n = 4p\left[\frac{|m|+1}{2} + \beta_n^{(0)} + \sum_{k=1}^{k_{\max}} \left(\frac{1}{4p}\right)^k \beta_n^{(k)}\right]. \tag{A.13}$$

Substituting (A.13) into (A.7) and equating the coefficients at equal powers of p, we arrive at the set of recurrence relations for evaluating the coefficients $\beta_n^{(k)}$ and $c_{s,n}^{(k)}$ (except $c_{0,n}^{(k)}$)

$$\begin{aligned} s c_{s,n}^{(k)} &= ((n+s+|m|+1)(2n+2s+|m|+1) - (n+s+|m|)(|m|+1))c_{s,n}^{(k-1)} \\ &\quad - (n+s)(n+s+|m|)c_{s-1,n}^{(k-1)} - (n+s+|m|+1)(n+s+1)c_{s+1,n}^{(k-1)} + \sum_{k'=1}^{k-|s|} \beta_n^{(k')} c_{s,n}^{(k-k')}, \end{aligned} \tag{A.14}$$

with the initial conditions

$$\beta_n^{(0)} = n, \qquad c_{s,n}^{(0)} = \delta_{s0}\sqrt{\frac{n!}{(n+|m|)!}}. \tag{A.15}$$

Note that all $c_{s,n}^{(k)} \equiv 0$ if $|s| > k$. For $k_{\max} = 1$ the output is the following:

$$\begin{aligned} c_{-1,n}^{(1)} &= n(n+|m|)c_{0,n}^{(0)}, \qquad \beta_n^{(1)} = -1 - 2n - 2|m|n - 2n^2 - |m|, \\ c_{1,n}^{(1)} &= -(n+1)(n+|m|+1)c_{0,n}^{(0)}. \end{aligned} \tag{A.16}$$

Substituting (A.13) into (A.12) and equating it to unity, we find the coefficients $c_{0,j}^{(k)}$

$$c_{0,n}^{(1)} = \frac{|m|(2n+|m|+1)}{2} c_{0,n}^{(0)}. \tag{A.17}$$

At step 6, substituting (A.13) with the coefficients $c_{s,j}^{(k)}$ evaluated at step 5 into the expressions of the matrix elements, evaluated at step 4 by means of equation (A.3), we easily find the matrix elements expanded in inverse powers of r with finite $j = n_l - 1$, $j' = n_r - 1$ and with the exponential terms omitted [22] in the form (71).

Appendix B. The effective approximation for the Kantorovich method

Consider the set of close-coupled radial equations (58) and neglect the coupling of the states $|j\rangle$ and $|j'\rangle$ disconnected from the open channel $|i_o\rangle$. This can be useful for sufficiently large effective charge $\hat{Z} = Z/\sqrt{\gamma}$, when the contribution of the adiabatic correction is sufficiently small. From the physical viewpoint this may help to understand the asymptotic boundary conditions in the open channel. We introduce the so-called effective adiabatic approximation, in which we project the radial equations onto the open channel $|i\rangle = |i_o\rangle$ by means of a canonical transformation. The new solution $\chi_{ii}^{\text{new}} \equiv \chi_{ii}^{\text{new}}(r)$ is related to the old solutions $\chi_{ji} \equiv \chi_{ji}(r)$ of equations (58) as

$$\chi_{ii}^{\text{new}} = \sum_j T_{ij}\chi_j \approx \sum_{j,j'=1}^{j_{\max}} \langle i|\exp(\imath S^{(2)})|j'\rangle\langle j'|\exp(\imath S^{(1)})|j\rangle\chi_{ji}. \tag{B.1}$$

Restricting the expansion of the exponentials to the second order $\exp(\imath S^{(1)}) \approx 1 + \imath S^{(1)} + (\imath S^{(1)})^2/2$ and $\exp(\imath S^{(2)}) \approx 1 + \imath S^{(2)}$, we define the nondiagonal matrix elements of the

generators $S^{(1)}$ and $S^{(2)}$ in the following way:

$$\begin{aligned}
&\imath S^{(1)}_{ij} = (1-\delta_{ij})\Delta^{-1}_{ij}\left(H_{ij} + Q_{ij}\frac{\mathrm{d}}{\mathrm{d}r} + \frac{1}{r^2}\frac{\mathrm{d}}{\mathrm{d}r}r^2 Q_{ij}\right),\\
&\imath S^{(2)}_{ij} = (1-\delta_{ij})2\Delta^{-2}_{ij}Q_{ij}V'_{jj},\\
&\Delta_{ij} = \Delta_{ij}(r) = V_{ii} - V_{jj}, \qquad V_{ii} = U_{ii}r^{-2}.
\end{aligned} \tag{B.2}$$

This approximation eliminates the rhs of equation (58) with the accuracy $O\left(\max_{ij}\left|\Delta^{-3}_{ij}\right|\right)$ and generates the inverse operator for the open channel $|i_o\rangle$

$$\begin{aligned}
&\chi_j = T^{-1}_{ji_o}\chi^{\mathrm{new}}_{i_o}, \qquad \chi^{\mathrm{new}}_{i_o} = \sum_j T_{i_o j}\chi_j,\\
&\langle i_o|T|i_o\rangle = \langle i_o|T^{-1}|i_o\rangle = 1 = \langle i_o|i_o\rangle.
\end{aligned} \tag{B.3}$$

As a result we get the projection of equations (58) onto the channel $|i_o\rangle$

$$\sum_{ij} T_{i_o i}(H^{\mathrm{old}} - 2E)_{ij}T^{-1}_{ji_o}\chi^{\mathrm{new}}_{i_o} = \left(H^{\mathrm{new}}_{i_o i_o} - 2E\right)\chi^{\mathrm{new}}_{i_o} = 0, \tag{B.4}$$

where

$$H^{\mathrm{new}}_{i_o i_o} = H^{\mathrm{old}}_{i_o i_o} + \tfrac{1}{2}[\imath S^{(1)}, H^{\mathrm{old}}]_{i_o i_o} + \tfrac{1}{2}[\imath S^{(1)} + \imath S^{(2)}, H^1]_{i_o i_o}, \tag{B.5}$$

and $H^1_{ij} = \Delta_{ij}\imath S^{(2)}_{ij}$. We can write equation (B.4) in the explicit form

$$-\frac{1}{r^2}\frac{\mathrm{d}}{\mathrm{d}r}\frac{r^2}{\mu(r)}\frac{\mathrm{d}\chi^{\mathrm{new}}_{i_o}(r)}{dr} + \frac{\mu'(r)}{\mu^2(r)r}\chi^{\mathrm{new}}_{i_o}(r) + [\hat{U}_{\mathrm{eff}} - 2E]\chi^{\mathrm{new}}_{i_o}(r) = 0. \tag{B.6}$$

The new solution $\psi \equiv \mu^{-1/2}\chi^{\mathrm{new}}_{ii}(r)$ in such a diagonal representation satisfies the following equation

$$-\frac{1}{r^2}(r^2\psi')' + \mu^{1/2}(\mu^{-1/2})''\psi + \mu[\hat{U}_{\mathrm{ad}} + \delta U - 2E]\psi = 0, \qquad \lim_{r\to 0} r^2\frac{\mathrm{d}\psi}{\mathrm{d}r} = 0, \tag{B.7}$$

where the modified scalar product and the adiabatic potential are defined as

$$\langle\psi|\psi\rangle = \int_0^\infty \mathrm{d}r r^2\mu\psi\psi, \qquad \hat{U}_{\mathrm{ad}} = V_{ii}.$$

The effective potential $\hat{U}_{\mathrm{eff}}(r)$ is the sum of the adiabatic potential $\hat{U}_{\mathrm{ad}}(r)$ and the *effective non-adiabatic correction* $\delta U(r)$. $\mu(r)$ can be considered as the *effective mass*, expressed as

$$\begin{aligned}
&\mu^{-1}(r) = 1 + W_{ii}(r), \qquad W_{ii}(r) = -4\sum_{j\neq i}^{j_{\max}} Q_{ij}(r)Q_{ji}(r)\Delta^{-1}_{ij}(r),\\
&\delta U(r) = \sum_{j\neq i}^{j_{\max}}\left(\Delta^{-1}_{ij}V^{(1)}_{ij} + \Delta^{-2}_{ij}V^{(2)}_{ij} + \Delta^{-3}_{ij}V^{(3)}_{ij}\right).
\end{aligned} \tag{B.8}$$

Here $W_{ii}(r)$ is the effective mass correction and

$$\begin{aligned}
&V^{(1)}_{ij} = H^2_{ij} - (Q'_{ij})^2 + 2Q_{ij}H'_{ij} - 2Q_{ij}Q''_{ij},\\
&V^{(2)}_{ij} = H_{ij}Q_{ij}(\Sigma'_{ij} - \Delta'_{ij}) + Q_{ij}Q'_{ij}(\Sigma'_{ij} + 3\Delta'_{ij}) + Q^2_{ij}(\Sigma''_{ij} + \Delta''_{ij}),\\
&V^{(3)}_{ij} = Q^2_{ij}(\Sigma'_{ij} + \Delta'_{ij})(\Sigma'_{ij} - 2\Delta'_{ij}),\\
&\Sigma_{ij} = \Sigma_{ij}(r) = V_{ii} + V_{jj}.
\end{aligned} \tag{B.9}$$

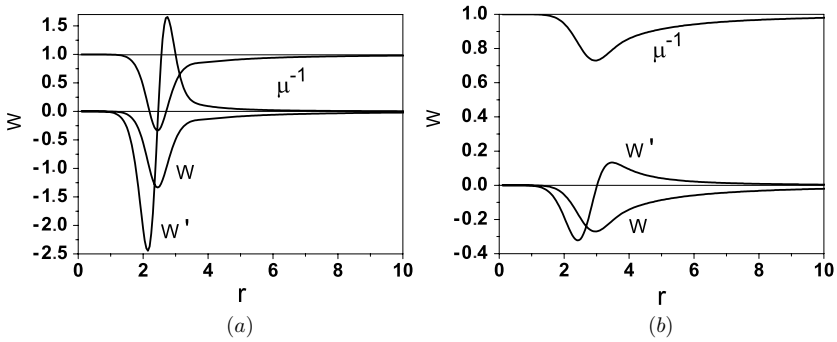

Figure B1. The effective mass correction W_{11}, its derivative W'_{11} and the inverse effective mass μ^{-1} at $\gamma = 1$ and $m = 0$ for the first even (a) and odd (b) states.

In the above expressions all terms are functions of r; the dash denotes the derivative with respect to r. At large r the leading terms of $W_{ii}(r)$ and $\delta U(r)$ calculated using the asymptotic basis functions read as

$$W_{ii}(r) = W_{ii}^{as} r^{-2} + O(r^{-4}), \qquad \delta U(r) = \delta U^{as} r^{-4} + O(r^{-6}), \tag{B.10}$$

where the effective mass correction

$$-W_{ii}^{as} = \langle i|\rho^2|i\rangle = 2(2n + |m| + 1)\gamma^{-1} \tag{B.11}$$

is the mean value of the transversal variable, $\rho^2 = (r\sin\theta)^2$, characterizing the electron precession around the z axis in the magnetic field γ(see figure 1), while

$$\delta U^{as} = -(4n^3 + 5n^2 - 4n - 3 + |m|(6n^2 + 5n - 2) + m^2(2n + 1))(2\gamma)^{-1} \tag{B.12}$$

is the asymptotic value correction of the electron polarizability,

$$U = U^{as} r^{-4} = (E^{(4)} + H^{(4)}) r^{-4}, \tag{B.13}$$

where coefficients $E^{(4)}$ and $H^{(4)}$ are given by (72) and (74). The plots of the above effective mass and effective potentials having essentially nonmonotonic behavior in a reaction region and given asymptotic form for large r are shown in figures B1 and B2.

For elastic scattering states with given $2E(p_{i_o}) = p_{i_o}^2 + E_{i_o}^{(0)}$ we reformulate the problem as

$$\left(\hat{H}_{\text{eff}} - p_{i_o}^2\right)\psi \equiv -\frac{1}{r^2}(r^2\psi')' + \mu^{1/2}(\mu^{-1/2})''\psi + \mu\left[\hat{U}_{\text{eff}} - 2E(p_{i_o})\right]\psi = 0. \tag{B.14}$$

For the function $\chi^{\text{eff}} = r\mu^{1/2}\psi$ this equation has the conventional form

$$\left(\frac{\mathrm{d}}{\mathrm{d}r}\mu^{-1}(r)\frac{\mathrm{d}}{\mathrm{d}r} - U_{\text{eff}}(r) + p_{i_o}^2\right)\chi_{i_o i_o}^{\text{eff}}(r) = 0, \tag{B.15}$$

where the effective potential is given by

$$U_{\text{eff}}(r) = V_{i_o i_o}(r) + \delta U(r) - \frac{2Z}{r} - E_{i_o}^{(0)}. \tag{B.16}$$

For large r, using the asymptotic values $W_{i_o i_o}^{(j_{\max})}$ of $r^2 W(r)$ and $\delta U_{i_o i_o}^{(j_{\max})}$ of $r^4\delta U(r)$ from (B.8) we have

$$\left(-\frac{\mathrm{d}}{\mathrm{d}r}\left(1 + \frac{W_{i_o i_o}^{(j_{\max})}}{r^2}\right)\frac{\mathrm{d}}{\mathrm{d}r} - \frac{2Z}{r} + \frac{\delta U_{i_o i_o}^{(j_{\max})}}{r^4} - p_{i_o}^2\right)\bar{\chi}_{i_o i_o}^{as}(r) = 0, \tag{B.17}$$

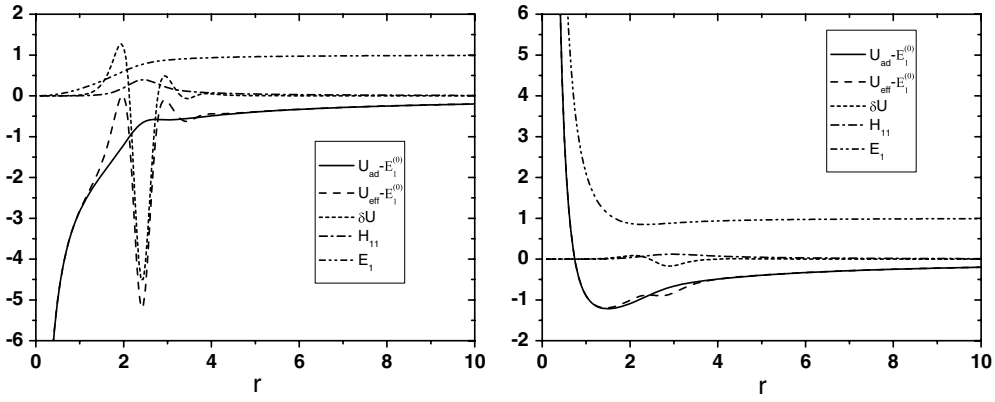

Figure B2. The adiabatic potential $\hat{U}_{\rm ad}(r)$, the effective adiabatic potential $\hat{U}_{\rm eff}(r)$, the effective non-adiabatic correction δU, the potential curve $E_1(r)$ and the radial potential H_{11} at $\gamma = 1$ and $m = 0$ for the first even (a) and odd (b) states.

and to the order of $O(r^{-3})$ equation (B.15) may be written as

$$\left(\frac{\mathrm{d}^2}{\mathrm{d}r^2} - \frac{2W_{i_oi_o}^{(j_{\max})}}{r^3}\frac{\mathrm{d}}{\mathrm{d}r} + \left(\frac{2Z}{r} + p_{i_o}^2\right)\left(1 - \frac{W_{i_oi_o}^{(j_{\max})}}{r^2}\right)\right)\bar{\chi}_{i_oi_o}^{as}(r) = 0. \tag{B.18}$$

For $p_{i_o}W_{i_oi_o}^{(j_{\max})}/(2r) \ll 1$ the solutions belonging to the continuous spectrum can be written in the form

$$\begin{aligned}\bar{\chi}_{i_oi_o}^{as}(r) &\approx \frac{1}{\sqrt{2\pi p_{i_o}}}\sin\left(p_{i_o}r_1 + \frac{Z}{p_{i_o}}\ln(2p_{i_o}r_1) + \delta^c + \delta^{(j_{\max})}\right)\\ &\approx \frac{1}{\sqrt{2\pi p_{i_o}}}\left[\sin\left(p_{i_o}r + \frac{Z}{p_{i_o}}\ln(2p_{i_o}r) + \delta^c + \delta^{(j_{\max})}\right)\right.\\ &\quad \left. + p_{i_o}\frac{W_{i_oi_o}^{(j_{\max})}}{2r}\cos\left(p_{i_o}r + \frac{Z}{p_{i_o}}\ln(2p_{i_o}r) + \delta^c + \delta^{(j_{\max})}\right)\right],\end{aligned} \tag{B.19}$$

where $r_1 = r\left(1 + W_{i_oi_o}^{(j_{\max})}/(2r^2)\right)$ and $r_1 = r(1 - \langle i_o|\rho^2|i_o\rangle/(2r^2))$ at $j_{\max} \geqslant i_o + 1$ and $\delta^{(j_{\max})} \equiv \delta^{(j_{\max})}\left(p_{i_o}\right)$ is the required phase shift of the elastic scattering in the open channel $|i_o\rangle$ count off the known Coulomb phase shift $\delta^c = \arg\Gamma\left(1 - \imath Z/p_{i_o}\right)$.

Remembering that $r^2 = \rho^2 + z^2$ and $|z| \sim r(1 - \rho^2/(2r^2))$ in the asymptotic region $\rho/r \ll 1$ one can introduce the *mean position* operator in the new representation $\chi^{\rm new} = T\chi$

$$r_{\rm mean}^{\rm new} = \left\langle\chi^{\rm new}\middle|\hat{r}_{\rm mean}^{\rm new}\middle|\chi^{\rm new}\right\rangle = \langle\chi|T^{-1}\hat{r}_{\rm mean}^{\rm new}T|\chi\rangle = \langle\chi|\hat{r}_{\rm mean}|\chi\rangle = r_{\rm mean}. \tag{B.20}$$

The *mean position* operator $\hat{r}_{\rm mean}^{\rm new} = r$ plays the role of the longitudinal coordinate z in the new representation $\chi^{\rm new}$. In other words, the z-delocalization is accounted for in the new radial functions $\chi^{\rm new} = T\chi$. In the old representation χ the mean position operator $\hat{r}_{\rm mean}$ is defined as

$$\hat{r}_{\rm mean} = T^{-1}\hat{r}_{\rm mean}^{\rm new}T = T^{-1}rT = r + \delta\hat{r}, \tag{B.21}$$

where $\delta\hat{r}$ is the delocalization of the longitudinal coordinate z that has the order of $\rho^2/(2r)$ in the asymptotic region $\rho/r \ll 1$ (see figure 1)

$$\hat{r}_{\rm mean} \to T^{-1}rT \approx \langle z\rangle. \tag{B.22}$$

Note that the transformation affects only the form of the radial solutions and the longitudinal coordinate z enters only the total expansion of the wavefunction. If we omit the non-adiabatic terms, the solution takes the adiabatic form

$$\chi^{\rm ad} \sim \sin\left(p_{i_o} r + \frac{Z}{p_{i_o}} \ln(2p_{i_o} r) + \delta^c + \delta^{\rm ad}\right). \tag{B.23}$$

Then the difference between the true phase shift δ, $j_{\max}$ th approximation $\delta^{(j_{\max})}$ and the adiabatic phase shift $\delta^{\rm ad}$ can be expressed as

$$\delta^{(j_{\max})} = \delta^{\rm ad} - p_{i_o} \frac{W^{(j_{\max})}_{i_o i_o}}{2r}, \qquad \delta = \lim_{j_{\max}\to\infty} \delta^{(j_{\max})} = \delta^{\rm ad} + p_{i_o} \frac{\langle i_o|\rho^2|i_o\rangle}{2r}. \tag{B.24}$$

The asymptotic solutions $\bar{\chi}_j(r)$ of equations (58) are related to the solution $\bar{\chi}^{\rm new}_{i_o i_o}(r)$ of the effective equation (B.7) via the inverse asymptotic transformation that reveals weak asymptotic coupling of the closed channels

$$\bar{\chi}^{as}_{ji_o}(r) = T^{-1}_{ji_o} \bar{\chi}^{\rm new}_{i_o i_o}(r) \sim \exp\left[-\frac{\langle j|\rho^2|i_o\rangle(1-\delta_{ji_o})}{2r} \frac{\rm d}{{\rm d}r}\right] \bar{\chi}^{\rm new}_{i_o i_o}(r). \tag{B.25}$$

Making use of equation (B.25), we arrive at the asymptotic solutions for equations (58)

$$\begin{aligned} \bar{\chi}^{as}_{i_o i_o}(r) = \bar{\chi}^{\rm new}_{i_o i_o}(r), \qquad \bar{\chi}^{as}_{ji_o}(r) &= T^{-1}_{j0} \bar{\chi}^{\rm new}_{i_o i_o}(r) \\ \approx -\frac{\langle j|\rho^2|i_o\rangle(1-\delta_{ji_o})}{2\sqrt{2\pi p_{i_o} r}} p_{i_o} \cos&\left(p_{i_o} r + \frac{Z}{p_{i_o}} \ln(2p_{i_o} r) + \delta^c + \delta^{(j_{\max})}\right). \end{aligned} \tag{B.26}$$

The expansion of the partial wavefunction Ψ_{i_o} in the open channel $|i_o\rangle$ over the set of asymptotic angular functions $\Phi_j(\theta; r) = r^{-1}\tilde{\Phi}_j(\rho)(1 + o(1))$ for $\rho/r \ll 1$,

$$\Psi_{i_o} = \left(\left|\tilde{\Phi}_{i_o}\right\rangle\left\langle\tilde{\Phi}_{i_o}\right|\tilde{\Phi}_{i_o}\right\rangle + \sum_{j\neq i_o}^{j_{\max}\to\infty} |\tilde{\Phi}_j\rangle\langle\tilde{\Phi}_j|T^{-1}\left|\tilde{\Phi}_{i_o}\right\rangle\right) \bar{\chi}^{\rm new}_{i_o i_o}(r), \tag{B.27}$$

subject to the completeness condition takes the form

$$\begin{aligned} \Psi_{i_o} \approx \frac{\tilde{\Phi}_{i_o}(\rho)}{\sqrt{2\pi p_{i_o}}} \Bigg[&\sin\left(p_{i_o} r + \frac{Z}{p_{i_o}} \ln(2p_{i_o} r) + \delta^c + \delta\right) \\ &- p_{i_o} \frac{\rho^2}{2r} \cos\left(p_{i_o} r + \frac{Z}{p_{i_o}} \ln(2p_{i_o} r) + \delta^c + \delta\right)\Bigg]. \end{aligned} \tag{B.28}$$

For $p_{i_o}\rho^2/(2r) \ll 1$, to the accuracy of $O(r^{-1})$, we have the true separable representation in cylindrical coordinates (ρ, z)

$$\begin{aligned} \Psi_{i_o}(r,\rho) &\sim \frac{\tilde{\Phi}_{i_o}(\rho)}{\sqrt{2\pi p_{i_o}}} \sin\left(p_{i_o}\left(r - \frac{\rho^2}{2r}\right) + \frac{Z}{p_{i_o}} \ln\left(2p_{i_o}\left(r - \frac{\rho^2}{2r}\right)\right) + \delta\left(p_{i_o}\right)\right) \\ &\to \frac{\tilde{\Phi}_{i_o}(\rho)}{\sqrt{2\pi p_{i_o}}} \sin\left(p_{i_o}|z| + \frac{Z}{p_{i_o}} \ln 2p_{i_o}|z| + \delta\left(p_{i_o}\right)\right) \sim \frac{\tilde{\Phi}_{i_o}(\rho)}{\sqrt{2\pi p_{i_o}}} \bar{\chi}^{(0)}_{i_o i_o}(|z|). \end{aligned} \tag{B.29}$$

Taking equation (56) and $|z| \sim r(1 - \rho^2/2r^2)$ into account, one can see that it is compatible with asymptotic expressions (75) and (81) to the order $k_{\max}$ of truncation of expansions (76) and (84).

Appendix C. Asymptotic function 'incident wave + ingoing wave'

Let us express the wavefunction (105) as

$$\Psi^{(-)}_{Em\vec{\leftarrow}}(r,\eta) = \tfrac{1}{\sqrt{2}}\left((\Phi^{m\sigma=+1}(\eta;r))^T\hat{\chi}^{(m\sigma=+1)}(E,r) \pm (\Phi^{m\sigma=-1}(\eta;r))^T\hat{\chi}^{(m\sigma=-1)}(E,r)\right)\exp(-\imath\delta^c). \tag{C.1}$$

As mentioned above, asymptotically this function consists of waves going into the center and an outgoing plane wave (reverse to the case of an incident plane wave and waves going out of the center in scattering theory). Using (57) equation (C.1) can be rewritten in the form

$$\Psi^{(-)}_{Em\vec{\leftarrow}}(r,\eta) = \tfrac{1}{2}\left((\Phi^{m\leftarrow}(\eta;r))^T[\hat{\chi}^{(m\sigma=+1)}(E,r) \pm \hat{\chi}^{(m\sigma=-1)}(E,r)] + (\Phi^{m\rightarrow}(\eta;r))^T[\hat{\chi}^{(m\sigma=+1)}(E,r) \mp \hat{\chi}^{(m\sigma=-1)}(E,r)]\right)\exp(-\imath\delta^c). \tag{C.2}$$

At $r\to\infty$, $|\eta|\sim 1$ it has the asymptotic form

$$\Psi^{(-)}_{Em\rightarrow}(r,\eta) \to \sqrt{\frac{2}{\pi}}((\Phi^{m\leftarrow}(\eta;r))^T[\check{\chi}(r)+\check{\chi}^*(r)\hat{\mathbf{R}}^\dagger] + (\Phi^{m\rightarrow}(\eta;r))^T\check{\chi}^*(r)\hat{\mathbf{T}}^\dagger), \tag{C.3}$$

$$\Psi^{(-)}_{Em\leftarrow}(r,\eta) \to \sqrt{\frac{2}{\pi}}((\Phi^{m\leftarrow}(\eta;r))^T\check{\chi}^*(r)\hat{\mathbf{T}}^\dagger + (\Phi^{m\rightarrow}(\eta;r))^T[\check{\chi}(r)+\check{\chi}^*(r)\hat{\mathbf{R}}^\dagger]), \tag{C.4}$$

where $\hat{\mathbf{T}}^\dagger$ and $\hat{\mathbf{R}}^\dagger$ are the conjugate transmission and reflection amplitude matrices from (31), and the fundamental solutions $\check{\chi}(r)$ are related to the asymptotic solutions $\chi(r)$ from (76) or (81)

$$\hat{\mathbf{T}}^\dagger = \tfrac{1}{2}\left(-\check{\mathbf{S}}^\dagger_{+1}+\check{\mathbf{S}}^\dagger_{-1}\right), \qquad \hat{\mathbf{R}}^\dagger = \tfrac{1}{2}\left(-\check{\mathbf{S}}^\dagger_{+1}-\check{\mathbf{S}}^\dagger_{-1}\right), \qquad \check{\chi}(r) = \chi(r)\exp(-\imath\delta^c). \tag{C.5}$$

Note that $\Phi^{m\leftarrow}(\eta;r) = \Phi^{m\rightarrow}(-\eta;r)$ and $\Phi^{m\leftarrow}(\eta<0;r) = \Phi^{m\rightarrow}(\eta>0;r) = O(\exp(-p(1+|\eta|))$ at $r\to\infty$ and $|\eta|\sim 1$. Equations (C.3) and (C.4) may be rewritten in the matrix form

$$\begin{pmatrix}\Psi^{(-)}_{Em\rightarrow}(r,\eta_+) & \Psi^{(-)}_{Em\leftarrow}(r,\eta_+)\\ \Psi^{(-)}_{Em\rightarrow}(r,\eta_-) & \Psi^{(-)}_{Em\leftarrow}(r,\eta_-)\end{pmatrix} \to \sqrt{\frac{2}{\pi}}\begin{pmatrix}\Phi^{m\leftarrow}(\eta_+;r) & 0\\ 0 & \Phi^{m\rightarrow}(\eta_-;r)\end{pmatrix}^T \times\left[\begin{pmatrix}\check{\chi}(r) & 0\\ 0 & \check{\chi}(r)\end{pmatrix}+\begin{pmatrix}0 & \check{\chi}^*(r)\\ \check{\chi}^*(r) & 0\end{pmatrix}\hat{\mathbf{S}}^\dagger\right], \tag{C.6}$$

where $\eta_\pm = \pm|\eta|$, $|\eta|\sim 1$ and $\hat{\mathbf{S}}^\dagger = \hat{\mathbf{S}}^{-1}$ is the inverse of the scattering matrix corresponding to (35):

$$\hat{\mathbf{S}}^\dagger = \begin{pmatrix}\hat{\mathbf{T}}^\dagger & \hat{\mathbf{R}}^\dagger\\ \hat{\mathbf{R}}^\dagger & \hat{\mathbf{T}}^\dagger\end{pmatrix}. \tag{C.7}$$

References

[1] Rotondi A *et al* 2005 *AIP Conf. Proc.* **796** 285–90
Madsen N *et al* 2005 *Phys. Rev. Lett.* **94** 033403-1–4
[2] Wetzels A, Gurtler A, Noordam L D and Robicheaux F 2006 *Phys. Rev.* A **73** 062507-1–8
[3] Menshikov L I and Landua R 2003 *Phys. Uspekhi* **46** 227–58
[4] Ryabinina M V and Melnikov L A 2005 *AIP Conf. Proc.* **796** 325–9
Ryabinina M V and Melnikov L A 2004 *Nucl. Instrum. Methods Phys. Res.* B **214** 35–9
[5] Serov V V, Derbov V L and Vinitsky S I 2007 *Opt. Spectrosc.* **102** 557–61
[6] Wang Q and Greene C H 1991 *Phys. Rev.* A **44** 7448–58
[7] Watanabe S and Komine H-A 1991 *Phys. Rev. Lett.* **67** 3227–30

[8] Zhao L B and Stancil P C 2006 *Phys. Rev.* A **74** 055401-1–4
[9] Dimova M G, Kaschiev M S and Vinitsky S I 2005 *J. Phys. B: At. Mol. Opt. Phys.* **38** 2337–52
[10] Abrashkevich A G and Shapiro M 1994 *Phys. Rev.* A **50** 1205–17
[11] Delande D, Bommier A and Gay J C 1991 *Phys. Rev. Lett.* **66** 141–4
[12] Eichler J, Yoshihama Y and Toshima N 2002 *Phys. Rev.* A **65** 033404-1–6
[13] Burke P G 1977 *Potential Scattering in Atomic Physics* (New York: Plenum)
[14] Fano U and Lee C M 1973 *Phys. Rev. Lett.* **31** 1573–6
[15] Lee C M 1974 *Phys. Rev.* A **10** 584–600
[16] Seaton M J 1983 *Rep. Prog. Phys.* **46** 167–257
[17] Greene C H 1983 *Phys. Rev.* A **28** 2209–16
[18] Kantorovich L V and Krylov V I 1964 *Approximate Methods of Higher Analysis* (New York: Wiley)
[19] Fano U 1977 *Colloq. Int. C. N. R. S.* **273** 127
Starace A F and Webster G L 1979 *Phys. Rev.* A **19** 1629–40
Clark C V, Lu K T and Starace A F 1984 *Progress in Atomic Spectroscopy* ed H G Beyer and H Kleinpoppen (New York: Plenum) Part C pp 247–320
[20] Abramovits M and Stegun I A 1972 *Handbook of Mathematical Functions* (New York: Dover) p 1037
[21] Chuluunbaatar O, Gusev A A, Derbov V L, Kaschiev M S, Serov V V, Tupikova T V and Vinitsky S I 2006 *Proc. SPIE* **6165** 61650B-1–17
[22] Vinitsky S I, Gerdt V P, Gusev A A, Kaschiev M S, Rostovtsev V A, Samoylov V N, Tupikova T V and Chuluunbaatar O 2007 *Program. Comput. Softw.* **33** 105–16
[23] Chuluunbaatar O, Gusev A A, Gerdt V P, Rostovtsev V A, Vinitsky S I, Abrashkevich A G, Kaschiev M S and Serov V V 2007 accepted in *Comput. Phys. Commun.*
[24] Damburg R J and Propin R Kh 1968 *J. Phys. B: At. Mol. Phys.* **1** 681–91
[25] Power J D 1973 *Phil. Trans. R. Soc.* A **274** 663–702
[26] Chuluunbaatar O, Gusev A A, Gerdt V P, Kaschiev M S, Rostovtsev V A, Samoylov V N, Tupikova T V and Vinitsky S I 2007 *Lect. Notes Comput. Sci.* at press
[27] Guest J R, Choi J-H and Raithel 2003 *Phys. Rev.* A **68** 022509-1–9
[28] Fridrich H 1982 *Phys. Rev.* A **46** 1827–38
[29] Alijah A, Hinze J and Broad J T 1990 *J. Phys. B: At. Mol. Opt. Phys.* **23** 45–60
[30] Gusev A A, Gerdt V P, Kaschiev M S, Rostovtsev V A, Samoylov V N, Tupikova T V and Vinitsky S I 2006 *Lecture Notes Comput. Sci.* **4194** 205–18
[31] Kaschiev M S, Vinitsky S I and Vukajlovic F R 1980 *Phys. Rev.* A **22** 557–559
[32] Gailitis M 1976 *J. Phys. B: At. Mol. Phys.* **9** 843–54
[33] Chuluunbaatar O, Gusev A A, Abrashkevich A G, Amaya-Tapia A, Kaschiev M S, Larsen S Y and Vinitsky S I 2007 *Comput. Phys. Commun.* (at press)
[34] http://physics.nist.gov/cuu/Constants/index.html
[35] Gusev A A, Samoilov V N, Rostovtsev V A and Vinitsky S I 2001 *CASC-2001: Proc. 4th Workshop on Computer Algebra in Scientific Computing* (Berlin: Springer) pp 309–22
[36] Seaton M J 2002 *Comput. Phys. Commun.* **146** 225–49
[37] Pupyshev V V 1995 *J. Phys. A: Math. Gen.* **28** 3305–18
Pupyshev V V 1997 *Phys. Part. Nucl.* **28** 586–614
[38] Sarkisyan H A 2002 *Mod. Phys. Lett.* B **16** 835–41
[39] Demkov Yu N and Meyer J D 2004 *Eur. Phys. J.* B **42** 361–5
[40] Kim J I, Melezhik V S and Schmelcher P 2006 *Phys. Rev. Lett.* **97** 193203-1–4